TECHNICAL MEMORANDUM

X-23

CHARACTERISTICS OF FIVE EJECTOR CONFIGURATIONS AT FREE-STREAM MACH NUMBERS FROM 0 TO 2.0

By John L. Klann and Ronald G. Huff

Lewis Research Center
Cleveland, Ohio

NATIONAL AERONAUTICS AND SPACE ADMINISTRATION
WASHINGTON

August 1959

NATIONAL AERONAUTICS AND SPACE ADMINISTRATION

TECHNICAL MEMORANDUM X-23

CHARACTERISTICS OF FIVE EJECTOR CONFIGURATIONS AT FREE-STREAM MACH NUMBERS FROM 0 TO 2.0*

By John L. Klann and Ronald G. Huff

SUMMARY

Thrust, air-handling, and base-pressure characteristics of five ejector configurations were investigated in the Lewis 8- by 6-foot wind tunnel at free-stream Mach numbers from 0 to 2.0 over ranges of primary-jet pressure ratio up to 24 and corrected secondary weight-flow ratio up to 13 percent. The ejector-shroud geometries varied from convergent to divergent.

Base pressure ratio and ejector performance were interrelated by means of an exit-momentum parameter. Correlations, to at least a first approximation, with base pressure ratio, of both internal-ejector-flow separation and external-flow separation over the model boattail were shown. Furthermore, it was shown that magnitudes and exact trends in base pressure ratio depended largely, and in a complicated fashion, on ejector geometry and amount of secondary flow.

External-stream effects on ejector jet thrust were determined for a typical schedule of jet-engine pressure ratios. With the exception of the ejector having the largest (1.81) shroud-exit- to primary-diameter ratio, there were no stream effects at Mach numbers from 1.5 to 2.0 and variations from quiescent-air thrust data were less than 2.5 percent at the subsonic speed investigated.

INTRODUCTION

Ejector jet-thrust and air-handling characteristics vary with ejector geometry, free-stream Mach number, and jet operating conditions. These characteristics are difficult to predict. Hence, several experimental investigations have been conducted to evaluate various ejector geometries. Reference 1 represents a rather thorough study of both cylindrical and divergent ejector-shroud geometries in quiescent air. However, it has been pointed out (ref. 2, e.g.) that quiescent-air data

*Title, Unclassified.

can overestimate the off-design performance of fixed-geometry ejectors at supersonic speeds. References 3 and 4 are typical of other investigations that have been conducted to evaluate external-stream effects on convergent-shroud ejector performance.

It was the purpose of this investigation to extend the evaluation of external-stream effects on ejector performance to shroud geometries of the divergent type. A series of five ejectors, three of which were similar to those of reference 1, were evaluated at Mach numbers of 0, 0.7, 1.5, 1.8, and 2.0. The investigation was conducted in the Lewis 8- by 6-foot wind tunnel over ranges of jet pressure ratio up to 24 and corrected weight-flow ratio up to 13 percent.

SYMBOLS

A	area, sq ft
A_{ex}	flow area at shroud exit, 0.117 sq ft
A_{ref}	momentum parameter reference area, 0.200 sq ft
$C_{D,bt}$	boattail drag coefficient based on maximum frontal area of 0.349 sq ft
D	diameter, in.
D_{ex}	diameter of flow passage at shroud exit, 4.632 in.
D_p	diameter of primary-nozzle exit, in.
D_s	diameter of secondary-flow passage at primary-nozzle exit, in.
F	jet thrust, lb
F_{ej}	ejector jet thrust, lb
$F_{p,id}$	ideal jet thrust for complete isentropic expansion of primary stream, lb
l	axial distance from primary-nozzle exit to shroud exit, in.
M	Mach number
m	mass flow, slugs/sec
P	total pressure, lb/sq ft

p	static pressure, lb/sq ft
P_p/p_0	jet pressure ratio
P_p/p_b	effective jet pressure ratio
P_s/P_p	ejector pressure ratio
T	total temperature, ^oR
V	velocity, ft/sec
w	weight flow, lb/sec
$\frac{w_s\sqrt{T_s}}{w_p\sqrt{T_p}}$	corrected weight-flow ratio
γ	ratio of specific heats
φ	nondimensional ejector exit-momentum parameter, $(F_{ej}+p_0A_{ex})/P_pA_{ref}$

Subscripts:

b	base of model
bt	boattail
d	design
ex	shroud exit
ext	external
fr	friction
int	internal
max	maximum
p	primary flow
q	quiescent air
s	secondary flow
sg	strain gage

w location on ejector shroud

0 free stream

APPARATUS AND PROCEDURE

Model

A sketch of the model is shown in figure 1. The nose cone was joined to an 8-inch-diameter cylinder at station 22.69. From station 55.44 to station 67.82, the model had a 4° boattail, while from the latter station to the shroud exit the boattail angle was increased to 12.5°.

The ejector configurations investigated are sketched in figure 2. Each ejector is described by three numbers: (1) shroud-exit- to primary-diameter ratio D_{ex}/D_p, (2) secondary- to primary-diameter ratio D_s/D_p, and (3) shroud-length to primary-diameter ratio l/D_p. (If $D_s/D_p > D_{ex}/D_p$, the shape of the shroud is convergent; if $D_s/D_p < D_{ex}/D_p$, it is divergent.) All these ejectors had the same shroud-exit diameter ($D_{ex} = 4.63$ in.). The first three sketches of figure 2 show a series of ejectors with shroud-exit- to primary-diameter ratios of 1.45, which vary only in secondary diameter. Nominal design pressure ratios based on shroud- to primary-exit area ratio are listed in the following table:

Ejector			Nominal design pressure ratio
D_{ex}/D_p	D_s/D_p	l/D_p	
1.30	1.65	0.80	8
1.45	1.80	.80	12
1.45	1.21	.80	12
1.45	1.09	.80	12
1.81	1.21	1.90	24

The 1.45-1.21-0.80, 1.45-1.09-0.80, and 1.81-1.21-1.90 ejector geometries are nearly similar to ejectors 1.44-1.21-1.06, 1.45-1.09-1.06, and 1.81-1.21-1.91, respectively, reported in reference 1.

Test Procedure

The investigation was conducted in the Lewis 8- by 6-foot wind tunnel at free-stream Mach numbers of 0, 0.7, 1.5, 1.8, and 2.0. Unheated and dried air was fed into the primary- and secondary-model passages through lateral support struts.

For the Mach 0 data of this investigation, a cone-cylinder "shield" was placed over the model (see fig. 1). With the shield in place, the wind tunnel was operated supersonically in order to lower the static pressure within the shield. With this device "quiescent-air" jet pressure ratios up to 21 could be obtained.

Instrumentation and Data Reduction

Thrust minus drag of the model was measured by the combination of a strain-gage balance and a pressurized bellows. The portion of the model attached to this combination is indicated in figure 1. The equations and forces considered in obtaining ejector jet thrust F_{ej} from the wind tunnel model are developed in the appendix. Methods used to obtain other parameters used in this investigation were as follows:

(1) Both secondary and primary total pressures were computed from measured weight flows, known areas, and the average of four static pressures in the straight section of each passage.

(2) Boattail pressure distributions were obtained from one longitudinal row of eight area-weighted static-pressure taps, while base pressures were averaged from four static-tap readings.

(3) Thermocouple readings in the primary and secondary passages were used with orifice measurements in calculating the corrected weight-flow ratio $w_s\sqrt{T_s}/w_p\sqrt{T_p}$.

(4) For the quiescent-air tests, four static orifices on the internal shield surface were used in determining the effective ambient pressure.

RESULTS AND DISCUSSION

Basic Data

Figures 3 to 7 present the air-handling, base-pressure, and jet-thrust characteristics of the ejectors of this investigation. These parameters are shown as functions of jet pressure ratio P_p/p_0 for approximately constant values (± 0.005) of corrected weight-flow ratio. In general, ejector jet-thrust measurements are believed to be accurate within 1 percent above jet pressure ratios of 10 and within 3 percent below 10. In one particular case these values are exceeded; it is believed that the entire thrust level of the convergent, 1.45-1.80-0.80 ejector with zero secondary flow (fig. 3(a)) was 2 or 3 percent too high.

It can be seen that, at the lower values of jet pressure ratio, both air-handling characteristics P_s/P_p and ejector jet-thrust ratio $F_{ej}/F_{p,id}$ depend on free-stream Mach number. This dependence, loosely called "stream effects", is controlled by the variation of base pressure ratio and the associated separation characteristics of the ejector.

Momentum Parameter

In analyzing an ejector, it would be desirable to have a parameter that will generalize performance independent of external Mach number. Such a parameter can be developed from the definition of ejector jet thrust. Written in the form

$$F_{ej} = \left[(mV)_{ex} + (pA)_{ex}\right] - (p_0 A_{ex})$$

the definition is made up of two terms, the first of which depends essentially on local pressure near the jet exit, namely base pressure p_b, and the second of which depends on free-stream static pressure p_0. Since the ratio between base pressure p_b and ambient pressure p_0 varies with stream Mach number (see figs. 3 to 7), F_{ej} may also vary, even though the ratio P_p/p_0 is held constant.

On the other hand, an exit-momentum parameter such as

$$\varphi \equiv \frac{(mV)_{ex} + (pA)_{ex}}{P_p A_{ref}}$$

should depend only on the effective jet pressure ratio P_p/p_b. For values of P_p/p_b above which the ejector flow is unseparated, φ should be constant. For lower values of effective jet pressure ratio, φ will vary; however, if the internal flow depends essentially on the effective jet pressure ratio, then φ will also depend on P_p/p_b, independent of stream Mach number.

Typical data are presented in terms of these more fundamental parameters in figures 8 and 9 at selected values of $w_s\sqrt{T_s}/w_p\sqrt{T_p}$. Also included is the variation of ejector pressure ratio P_s/P_p. It can be seen that, while the ejectors are unseparated, both P_s/P_p and φ are constant, and in addition that over the entire range both are functions of P_p/p_b only.

The properties of the exit-momentum parameter were originally used to more readily detect errors which arose in the large number of terms

for obtaining ejector jet thrust (see appendix). Failure of the data to exhibit trends similar to those of figures 8 and 9 indicated errors. But, it should also be noted that the properties of this momentum parameter could be used to estimate performance of the ejector with external flow from its quiescent performance. From previously published data, base pressures for most geometries could be at least estimated. Then with quiescent-air results and the equation

$$F_{ej} = P_p A_{ref}(\varphi) - p_0 A_{ex}$$

ejector performance at stream Mach numbers could be obtained.

In general, however, the examples shown here stress the large dependence of nozzle performance on base pressure. The correlation of φ with effective jet pressure ratio has implied that, to at least a first approximation, base pressure controlled internal-ejector-flow separation.

Base Pressure

Effect of jet pressure ratio. - At the subsonic speed tested ($M_0 = 0.7$) base pressure ratios were generally near unity; at supersonic speeds, however, large variations in base pressure ratio occurred with both stream Mach number and jet pressure ratio.

For all ejectors, as jet pressure ratio increased, base pressure first generally decreased, reached a minimum, and then increased. This trend is similar to that observed for nonejector nozzle types (e.g., ref. 5).

The minimum base pressure occurs at or near the jet pressure ratio for which the internal flow just fills the shroud. This is illustrated in figure 10. Base- and nozzle-exit-pressure ratios are plotted as functions of jet pressure ratio for configuration 1.81-1.21-1.90. The exit pressure ratio is actually the ratio of shroud-wall static pressure near the exit station to primary total pressure and, therefore, can be used as an indication of exit flow conditions. Thus, if exit pressure ratio is constant and independent of jet pressure ratio, the nozzle flow is fully expanded. Comparison of the base- and exit-pressure ratios shows that at all three Mach numbers the minimum base pressure occurred at jet pressure ratios very close to those for which the ejector flow was just fully expanded.

In the region of low jet pressure ratio, where base pressure decreases with increasing jet pressure ratio, the internal flow is not fully expanded, and the exact trend of base pressure depends greatly on the separation characteristics of the nozzle, that is, on factors such as shroud shape, design pressure ratio, and amount of secondary flow.

Effect of secondary flow. - Typical effects of secondary flow on base pressure are shown in figure 11. Base pressure trends with secondary flow are complicated and depend greatly on ejector geometry. This fact is exemplified in this figure where large variations in base pressure ratio occurred for small changes in corrected weight-flow ratio in the 1.45-1.21-0.80 configuration at a Mach number of 1.8, while little effect was observed, for example, in the 1.45-1.09-0.80 and 1.81-1.21-1.90 ejectors at Mach 2.0.

Effect of base pressure on boattail drag. - Base pressure ratio not only controls separation of internal ejector flow, but is also a parameter controlling external-flow separation over the boattail of the model. In figure 12, boattail drag is presented as a function of base pressure ratio for the four stream Mach numbers investigated. At each supersonic Mach number and for low base pressure ratios, boattail drag was constant. In each of these cases, a base pressure ratio existed above which external separation occurred. Base pressure could then feed upstream along the boattail, and hence boattail drag decreased.

Stream Effects

Figure 13 presents the deviation between ejector jet thrust at the four stream Mach numbers investigated and quiescent jet thrust. The abscissa in this figure has been generalized to fractions of the nominal design pressure ratios. In general, all stream effects on ejector jet thrust occurred below 0.6 of the design jet pressure ratios. From the data shown in figure 13, it can be seen that the Mach 1.8 and 2.0 trends were similar, with thrusts always less than those in quiescent air. The Mach 0.7 and 1.5 data show variations that, in general, were smaller than those shown by the Mach 1.8 and 2.0 data. In quite a few cases (e.g., zero weight flow, fig. 13(e)) it can be seen that quiescent-air thrust measurements would underestimate Mach 0.7 and 1.5 ejector performance.

A typical schedule of jet-engine pressure ratios has been assumed in order to illustrate stream effects on these ejectors at their normal operating points. Ejector operating conditions are indicated on the curves of figure 13 according to the following schedule:

Free-stream Mach number	Jet pressure ratio
0.7	3.5
1.5	6
1.8	8
2.0	10

For all ejectors, except the 1.81-1.21-1.90 configuration with zero secondary flow, there would be no stream effects on thrust performance at Mach numbers of 1.5, 1.8, and 2.0. In the case of the exception, quiescent data would overestimate jet thrust performance at Mach 1.5 by 2.5 percent, at Mach 1.8 by 1.5 percent, and at Mach 2.0 by less than 1 percent.

Quiescent data would tend to underestimate Mach 0.7 ejector performance. All stream effects at this subsonic Mach number would be less than 2.5 percent of quiescent results except, again, for the 1.81-1.21-1.90 configuration, where 15.5- and 5.5-percent underestimation would occur for corrected weight-flow ratios of 0 and 0.03, respectively.

In general, stream effects occur only for highly overexpanded ejector operation. Hence, these effects would be important for fixed-geometry, high-design-Mach-number ejectors operating at off-design conditions.

SUMMARY OF RESULTS

Thrust, air-handling, and base-pressure characteristics of five ejector configurations were investigated at free-stream Mach numbers from 0 to 2.0. Ejector shroud geometries varied from convergent to divergent.

Base pressure ratio was demonstrated to be an important factor controlling ejector performance. The data shown herein indicated base pressure correlations, to at least a first approximation, of both internal-ejector-flow separation and external-flow separation over the model boattail. Ejector jet thrust at any free-stream Mach number could be obtained from quiescent-air results, if the values of base pressure ratio could be estimated. It was shown that magnitudes and exact trends in base pressure ratio depended largely on ejector geometry and amount of secondary flow.

For a typical schedule of jet-engine pressure ratios, no stream effects on jet thrust were observed at Mach numbers from 1.5 to 2.0, except for the ejector with the largest exit- to primary-diameter ratio (1.81) with zero secondary flow. Mach 0.7 ejector thrust performance tended to be underestimated by the quiescent results.

Lewis Research Center
National Aeronautics and Space Administration
Cleveland, Ohio, March 31, 1959

APPENDIX - FORCE REDUCTION

From the summation of forces acting on the model (see sketch for definition of symbols),

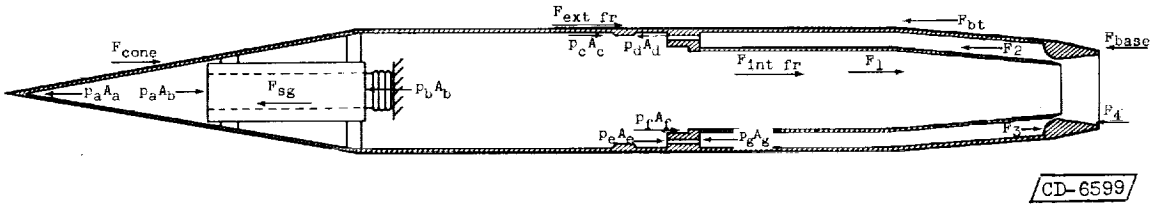

$$\sum F_{axial} = 0$$

$$F_{sg} + (p_b - p_a)A_b + F_{int} - \int_{cone} pdA + \int_{boattail} pdA + \int_{base} pdA -$$

$$F_{int\ fr} - F_{ext\ fr} - F_1 + F_2 - F_3 + F_4 = 0 \qquad (1)$$

where

$$F_{int} = p_a A_a - p_c A_c + p_d A_d - p_e A_e - p_f A_f + p_g A_g$$

But by definition,

$$F_{ej} \equiv \left[mV + (p - p_0)A\right]_{exit} \qquad (2)$$

$$D_0 \equiv \int_{cone} (p - p_0)dA + F_{ext\ fr} = \int_{cone} pdA - p_0 A_{max} + F_{ext\ fr} \qquad (3)$$

$$D_{bt} = \int_{boattail} (p_0 - p)dA = p_0 A_{bt} - \int_{boattail} pdA \qquad (4)$$

$$D_{base} = \int_{base} (p_0 - p)dA = p_0 A_b - \int_{base} pdA \qquad (5)$$

Expanding a portion of equation (2) yields

$$(mV + pA)_{exit} = [pA(1 + \gamma M^2)]_{exit}$$

$$= p_s A_s(1 + \gamma M_s^2) + p_p A_p(1 + \gamma M_p^2) -$$

$$F_1 + F_2 - F_3 + F_4 - F_{int\ fr} \qquad (6)$$

where the momentum is evaluated at upstream constant-area sections of the primary and secondary passages.

Substituting equations (2) to (6) into equation (1) and noting that

$$A_{max} = A_{ex} + A_{base} + A_{bt} \qquad (7)$$

results in the working equation for ejector jet thrust

$$F_{ej} = D_0 + D_{bt} + D_{base} + p_s A_s(1 + \gamma M_s^2) +$$

$$p_p A_p(1 + \gamma M_p^2) - F_{int} - F_{sg} - (p_b - p_a)A_b \qquad (8)$$

REFERENCES

1. Greathouse, William K., and Beale, William T.: Performance Characteristics of Several Divergent-Shroud Aircraft Ejectors. NACA RM E55G21a, 1955.

2. Valerino, Alfred S., and Yeager, Richard A.: External-Stream Effects on Gross Thrust and Pumping Characteristics of Ejectors Operating at Off-Design Mach Numbers. NACA RM E56C14, 1956.

3. Hearth, Donald P., and Valerino, Alfred S.: Thrust and Pumping Characteristics of a Series of Ejector-Type Exhaust Nozzles at Subsonic and Supersonic Flight Speeds. NACA RM E54H19, 1954.

4. Stitt, Leonard E., and Valerino, Alfred S.: Effect of Free-Stream Mach Number on Gross-Force and Pumping Characteristics of Several Ejectors. NACA RM E54K23a, 1955.

5. Baughman, L. Eugene, and Kochendorfer, Fred D.: Jet Effects on Base Pressures of Conical Afterbodies at Mach 1.91 and 3.12. NACA RM E57E06, 1957.

[redacted]

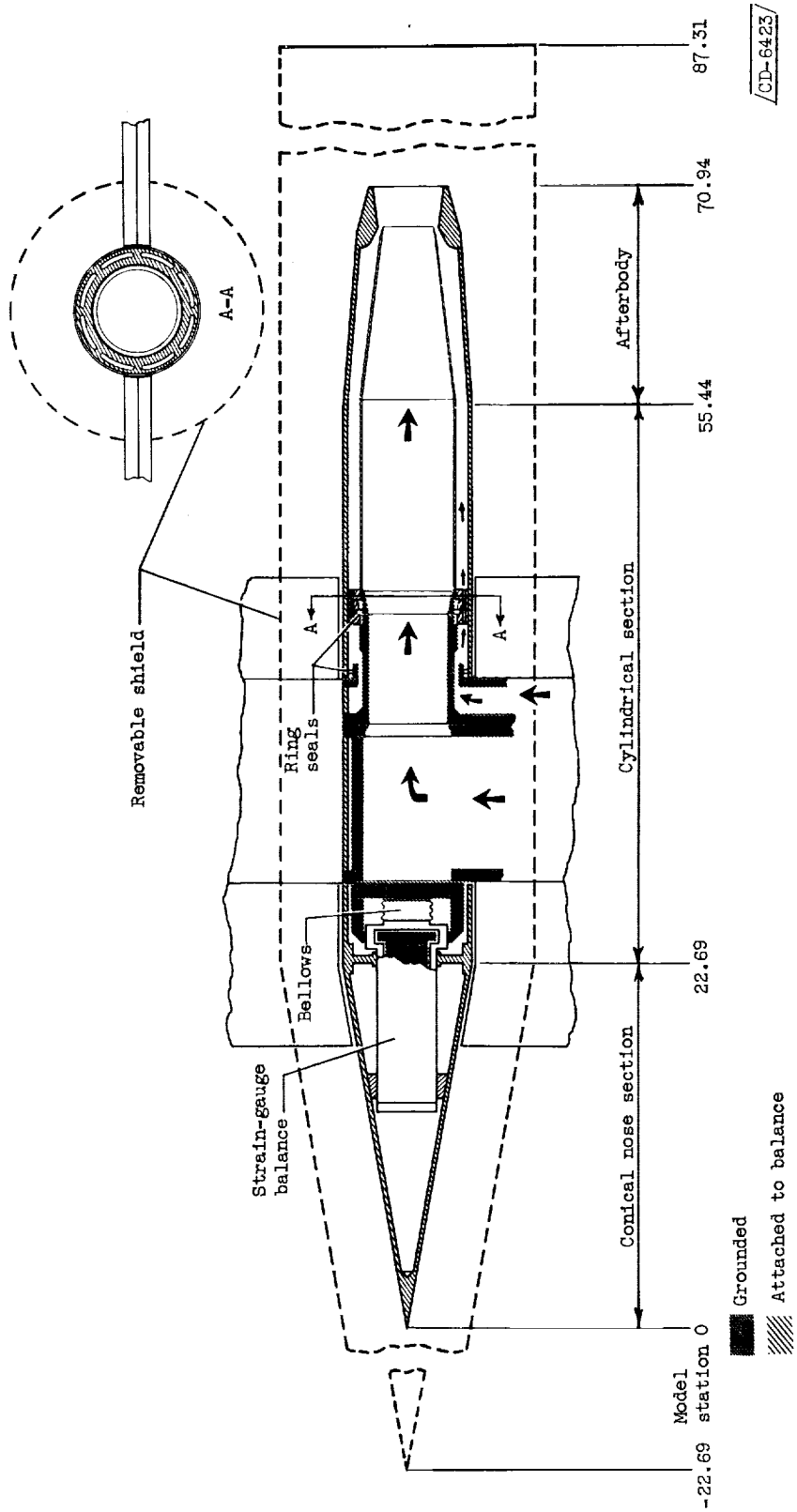

Figure 1. - Schematic diagram of jet-exit model.

[redacted]

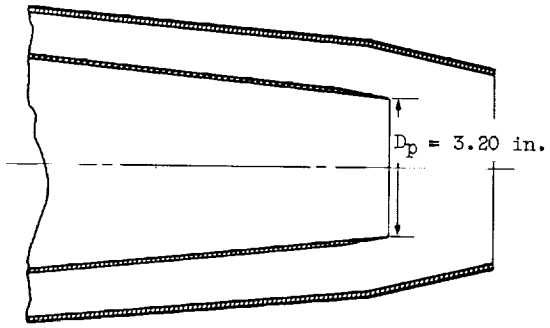

(a) Ejector 1.45-1.80-0.80.
(Basic data in fig. 3.)

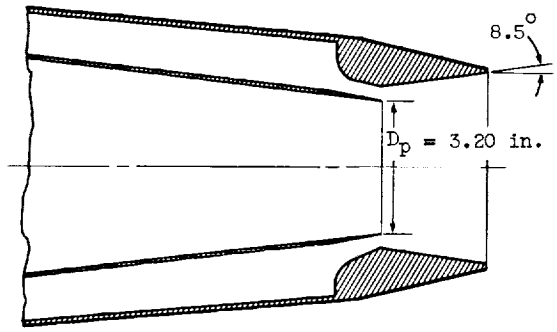

(b) Ejector 1.45-1.21-0.80.
(Basic data in fig. 4.)

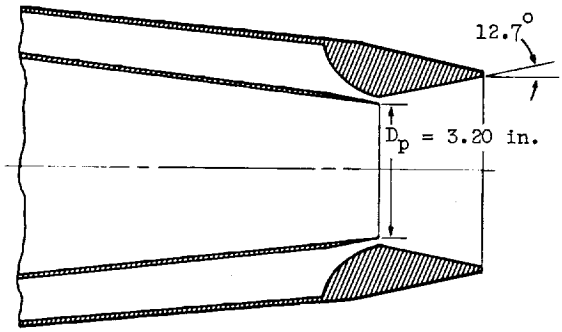

(c) Ejector 1.45-1.09-0.80.
(Basic data in fig. 5.)

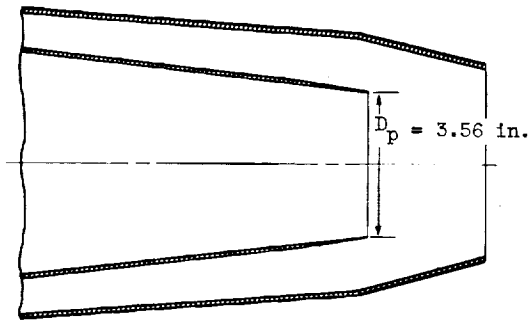

(d) Ejector 1.30-1.65-0.80.
(Basic data in fig. 6.)

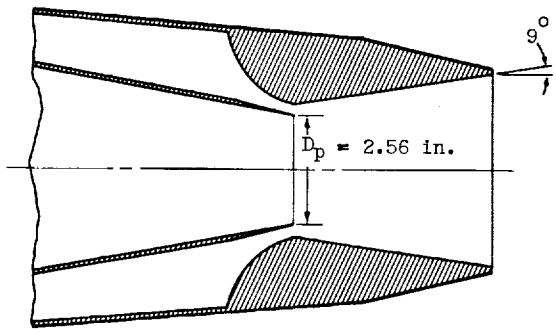

(e) Ejector 1.81-1.21-1.90.
(Basic data in fig. 7.)

CD-6596

Figure 2. - Ejector configurations. (Each ejector described by values of D_{ex}/D_p, D_s/D_p, and l/D_p, respectively.)

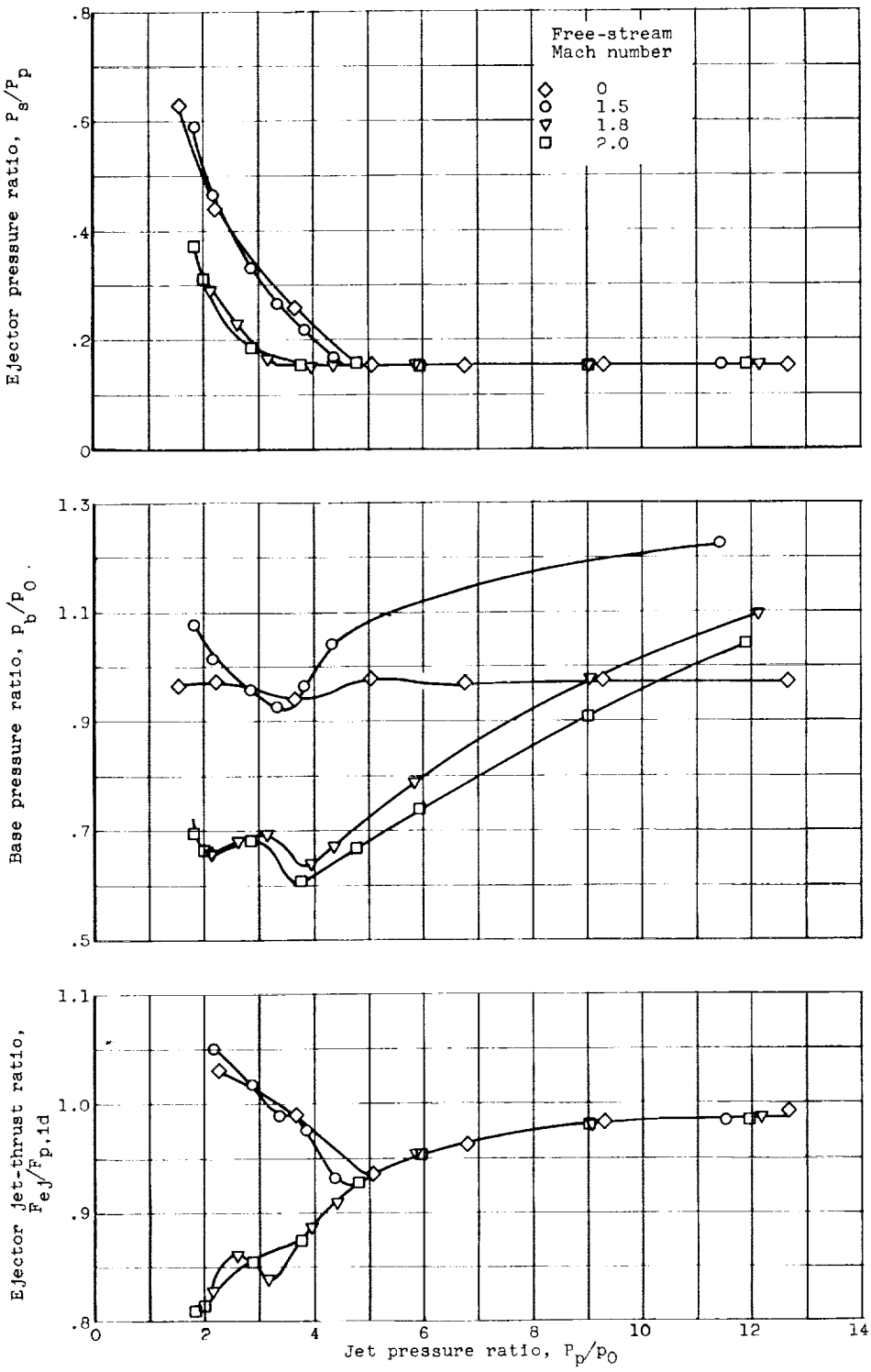

(a) Corrected weight-flow ratio, 0

Figure 3. - Air-handling, base-pressure, and jet-thrust variations with jet pressure ratio for ejector 1.45-1.80-0.80.

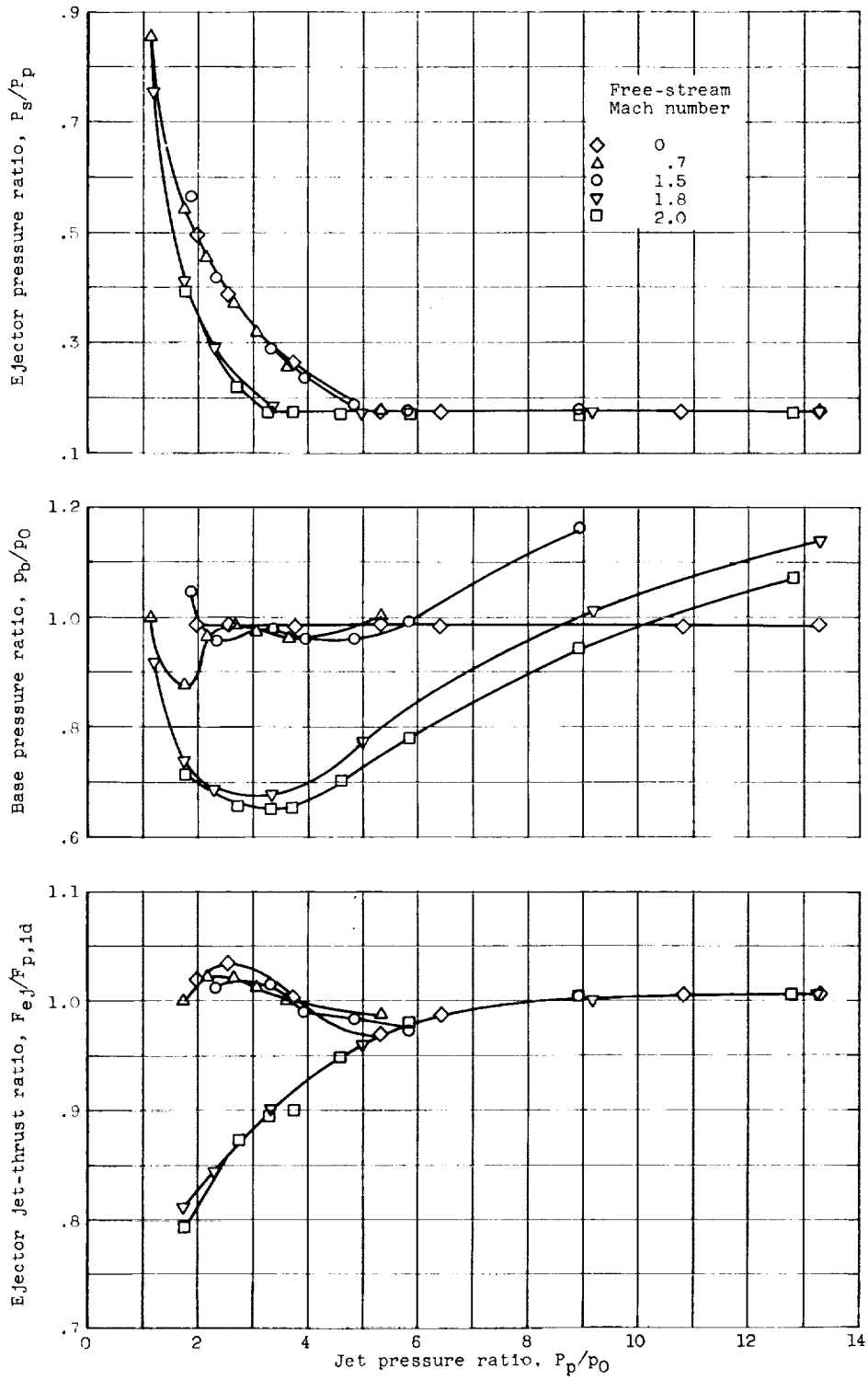

(b) Corrected weight-flow ratio, 0.03.

Figure 3. - Continued. Air-handling, base-pressure, and jet-thrust variations with jet pressure ratio for ejector 1.45-1.80-0.80.

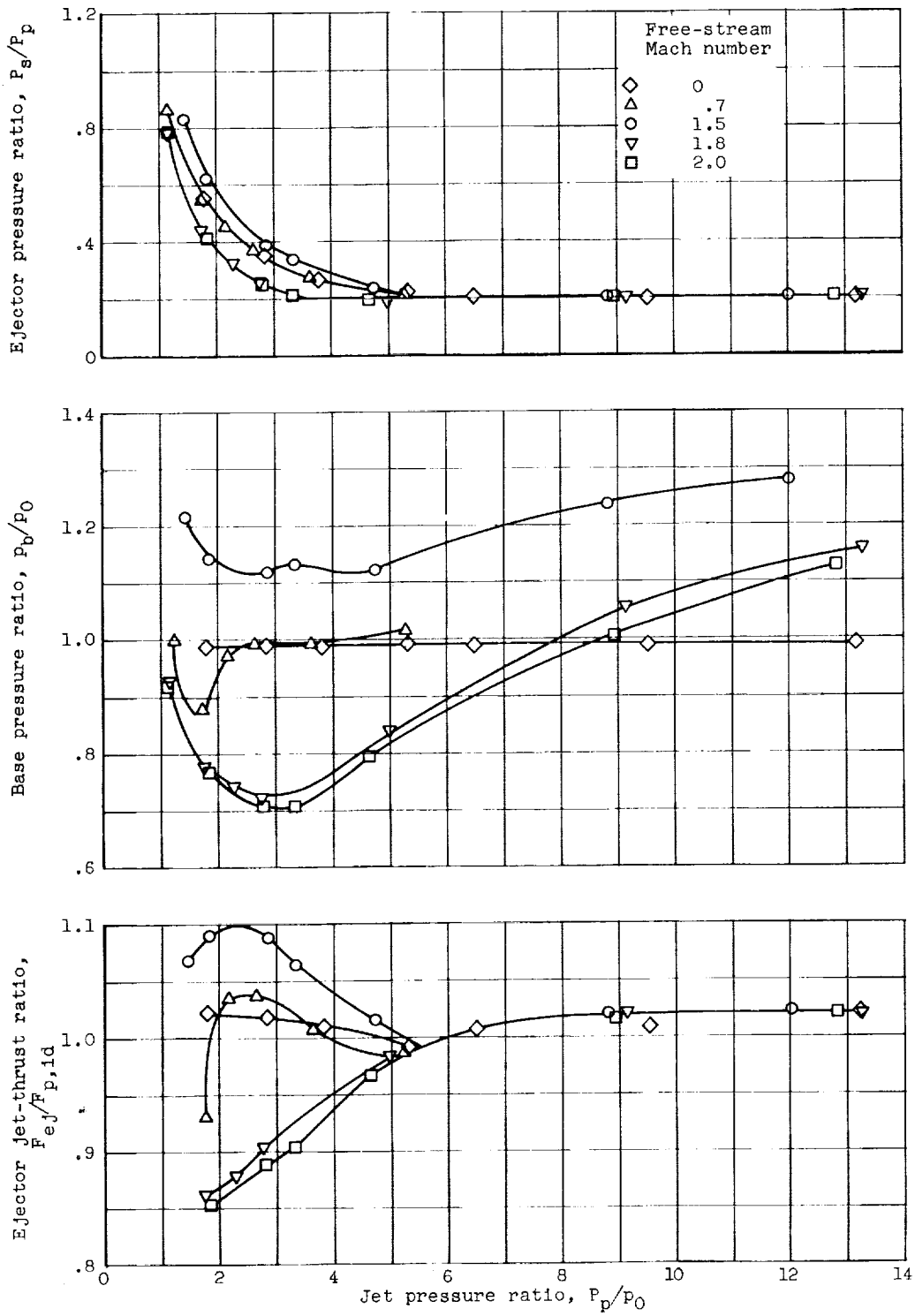

(c) Corrected weight-flow ratio, 0.06.

Figure 3. - Continued. Air-handling, base-pressure, and jet-thrust variations with jet pressure ratio for ejector 1.45-1.80-0.80.

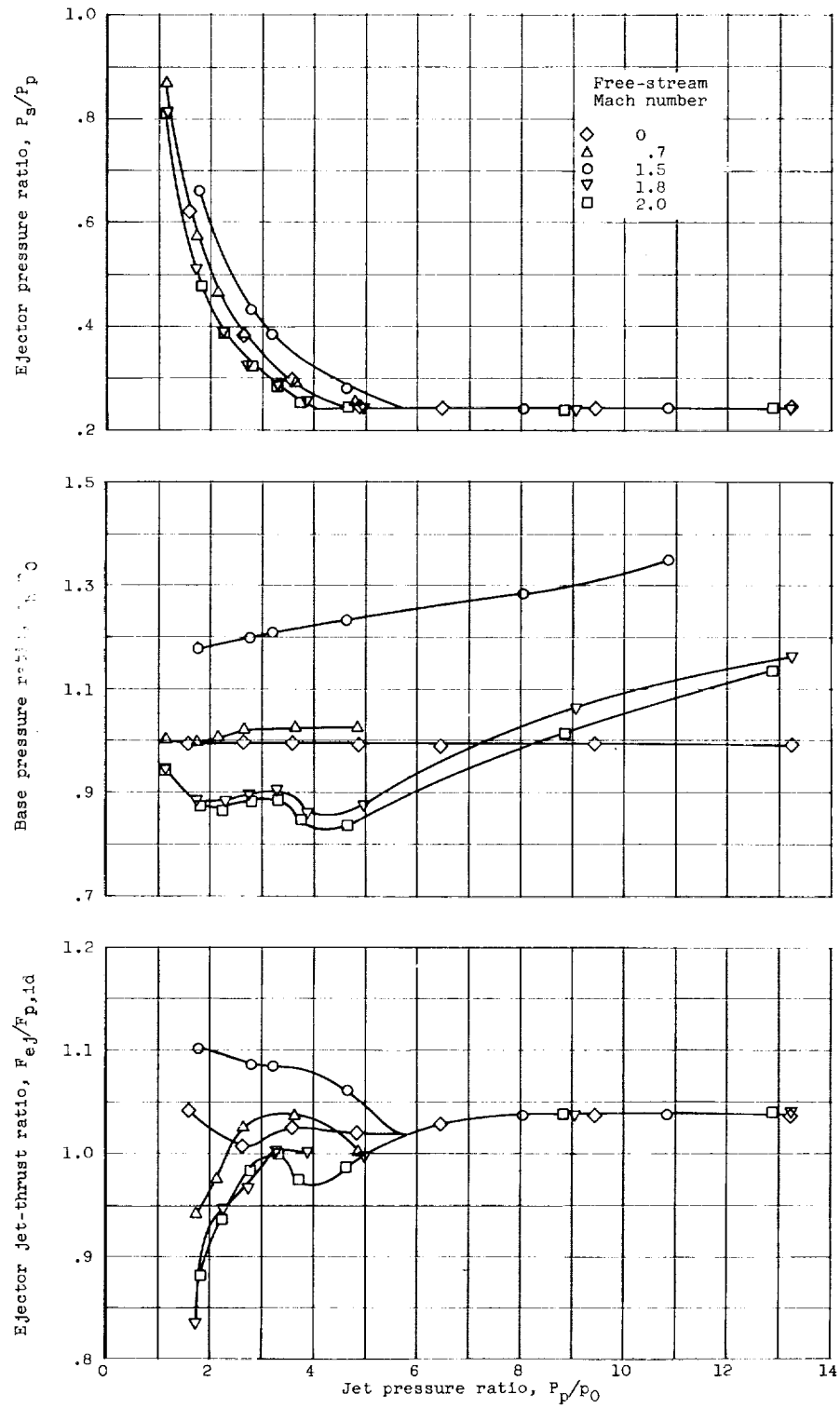

(d) Corrected weight-flow ratio, 0.12.

Figure 3. - Concluded. Air-handling, base-pressure, and jet-thrust variations with jet pressure ratio for ejector 1.45-1.80-0.80.

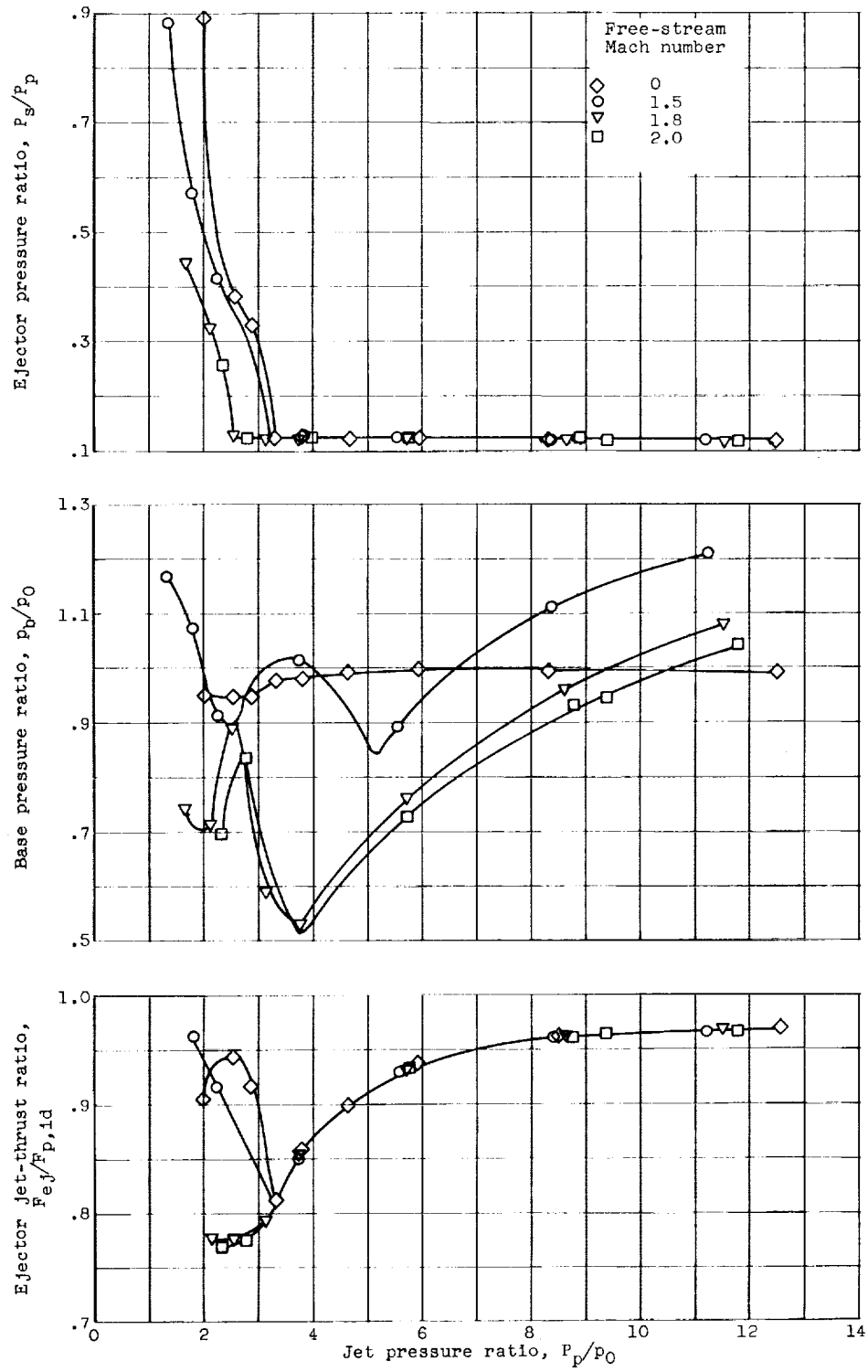

(a) Corrected weight-flow ratio, 0.01.

Figure 4. - Air-handling, base-pressure, and jet-thrust variations with jet pressure ratio for ejector 1.45-1.21-0.80.

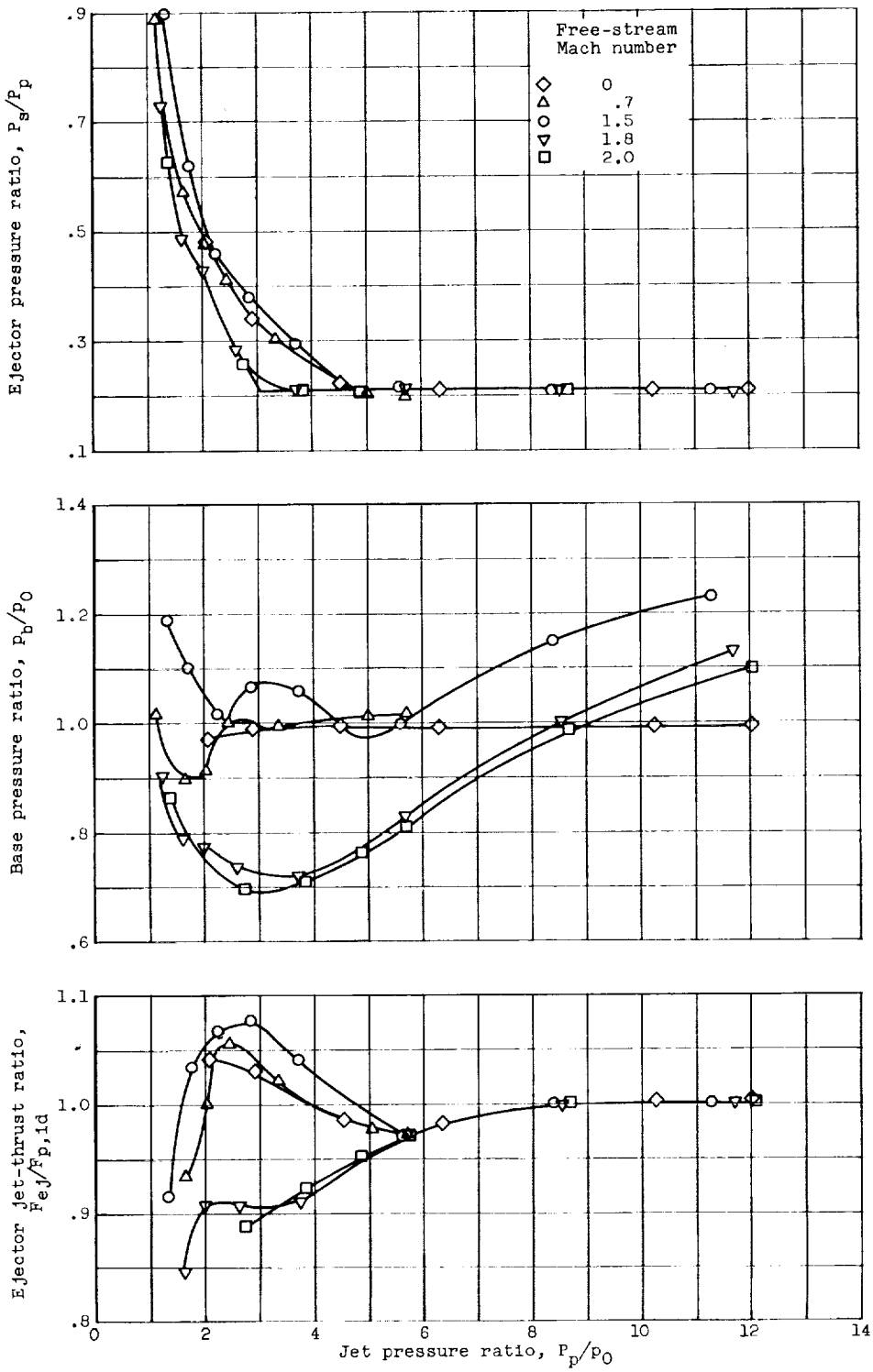

(b) Corrected weight-flow ratio, 0.03

Figure 4. - Continued. Air-handling, base-pressure, and jet-thrust variations with jet pressure ratio for ejector 1.45-1.21-0.80.

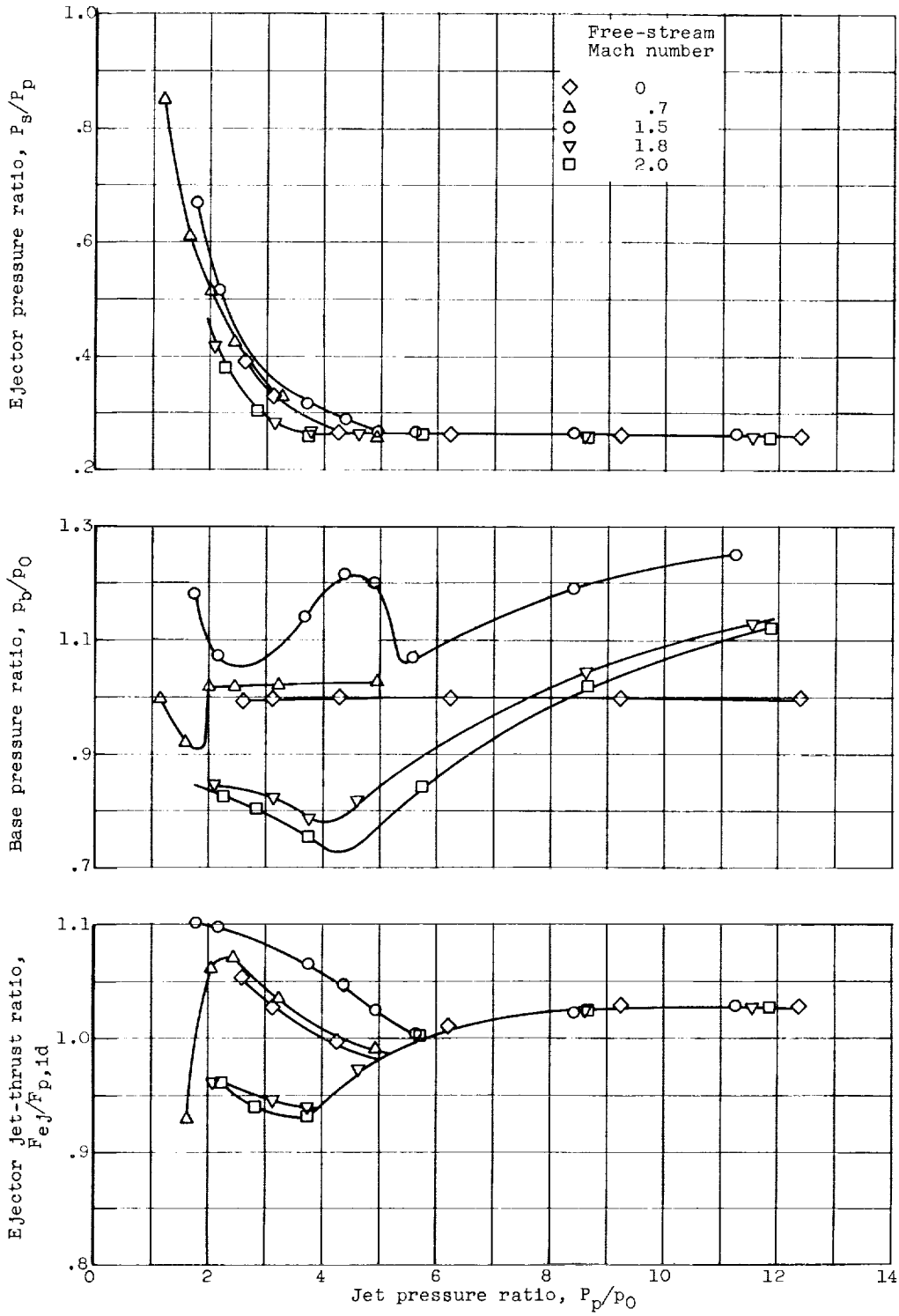

(c) Corrected weight-flow ratio, 0.05.

Figure 4. - Continued. Air-handling, base-pressure, and jet-thrust variations with jet pressure ratio for ejector 1.45-1.21-0.80.

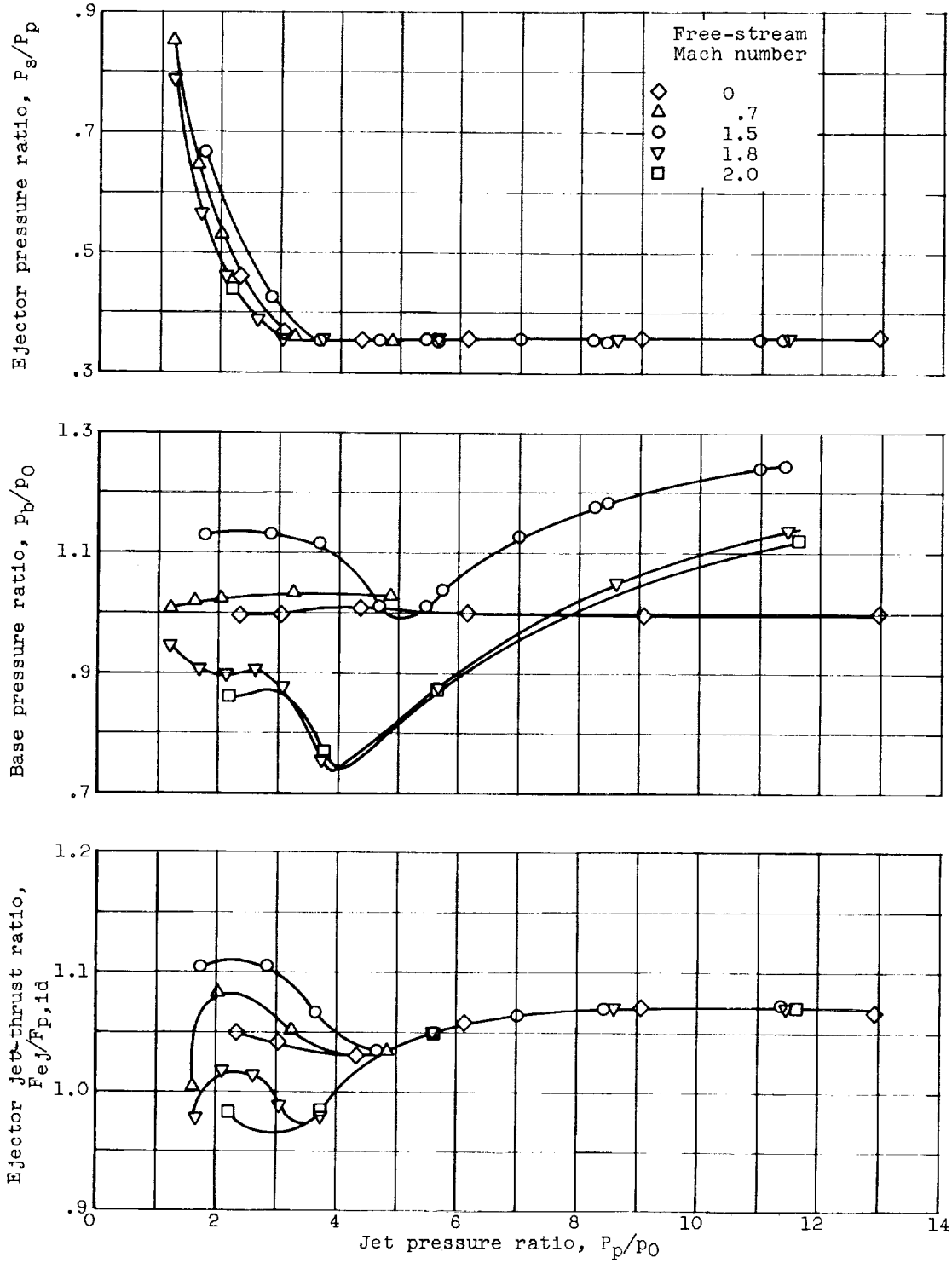

(d) Corrected weight-flow ratio, 0.09.

Figure 4. - Concluded. Air-handling, base-pressure, and jet-thrust variations with jet pressure ratio for ejector 1.45-1.21-0.80.

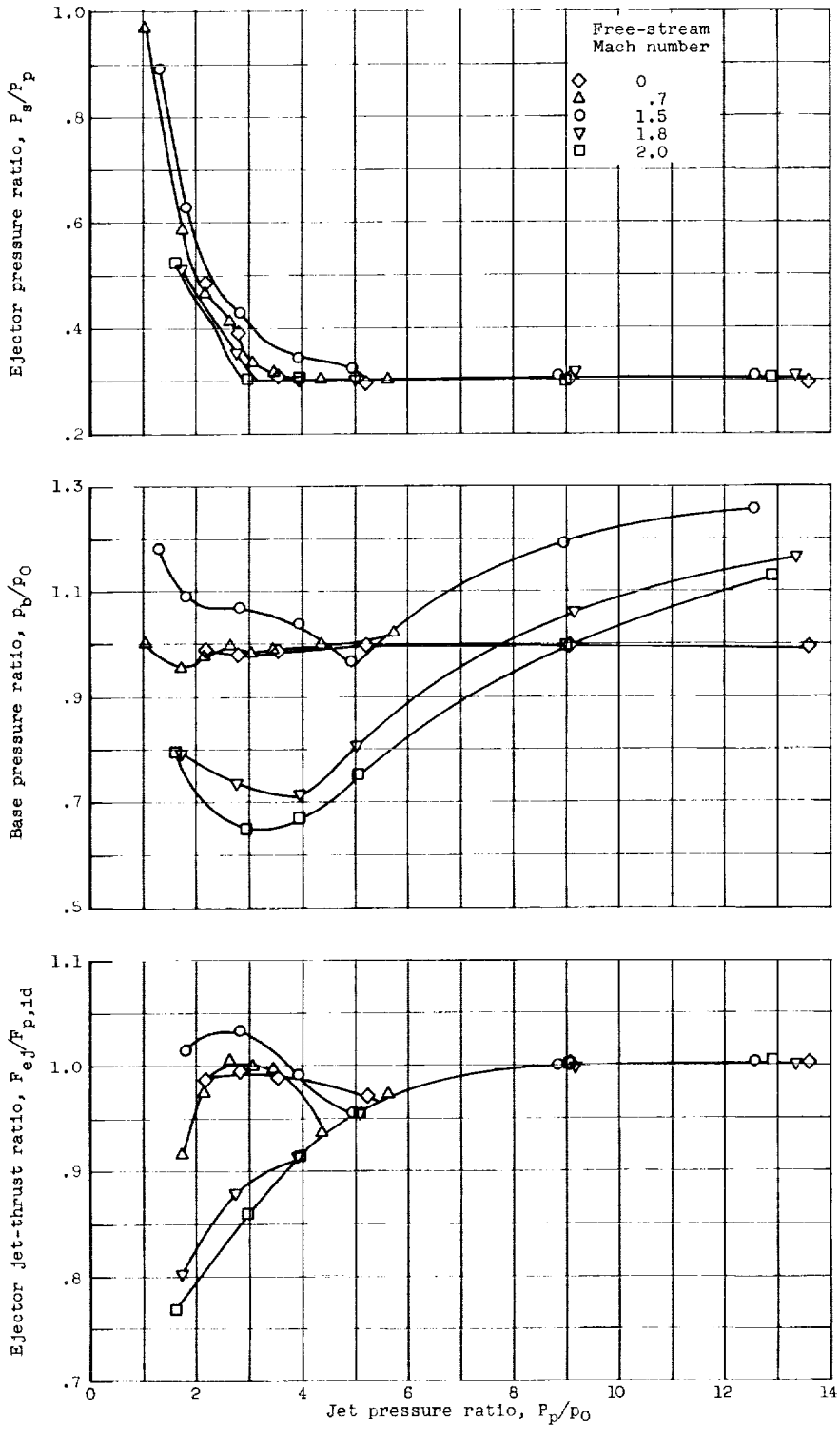

(a) Corrected weight-flow ratio, 0.03.

Figure 5. - Air-handling, base-pressure, and jet-thrust variations with jet pressure ratio for ejector 1.45-1.09-0.80.

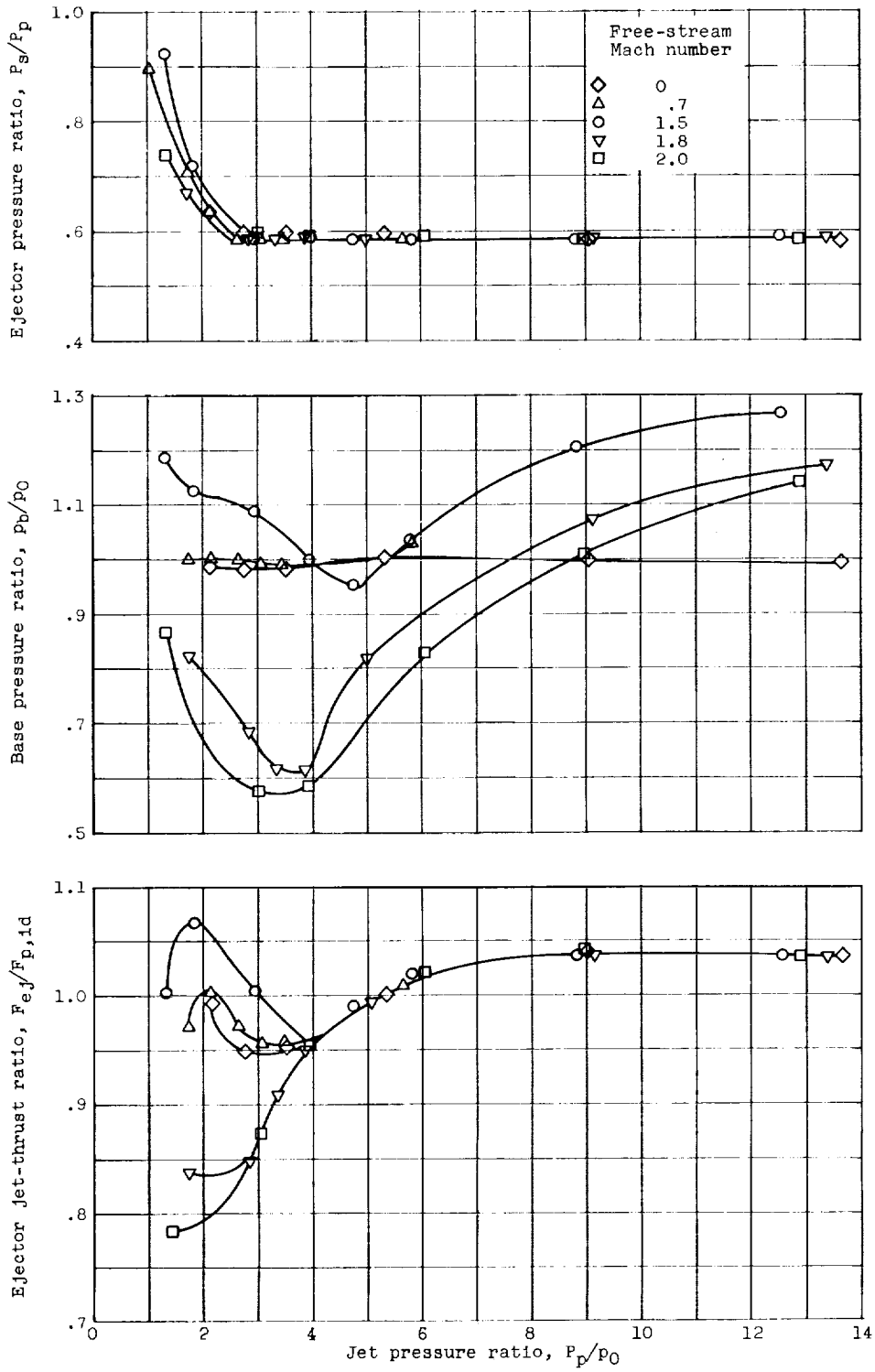

(b) Corrected weight-flow ratio, 0.06.

Figure 5. - Concluded. Air-handling, base-pressure, and jet-thrust variations with jet pressure ratio for ejector 1.45-1.09-0.80.

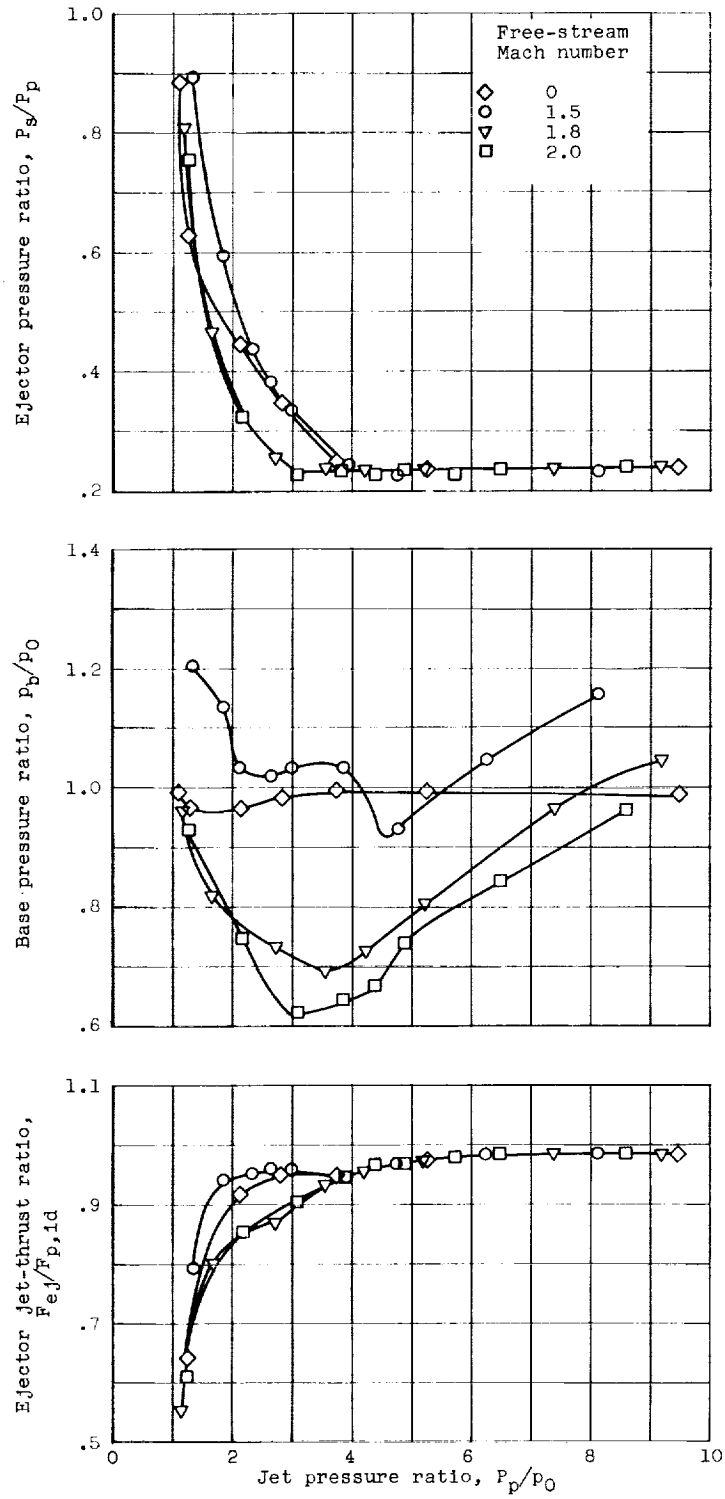

(a) Corrected weight-flow ratio, 0.03.

Figure 6. - Air-handling, base-pressure, and jet-thrust variations with jet pressure ratio for ejector 1.30-1.65-0.80.

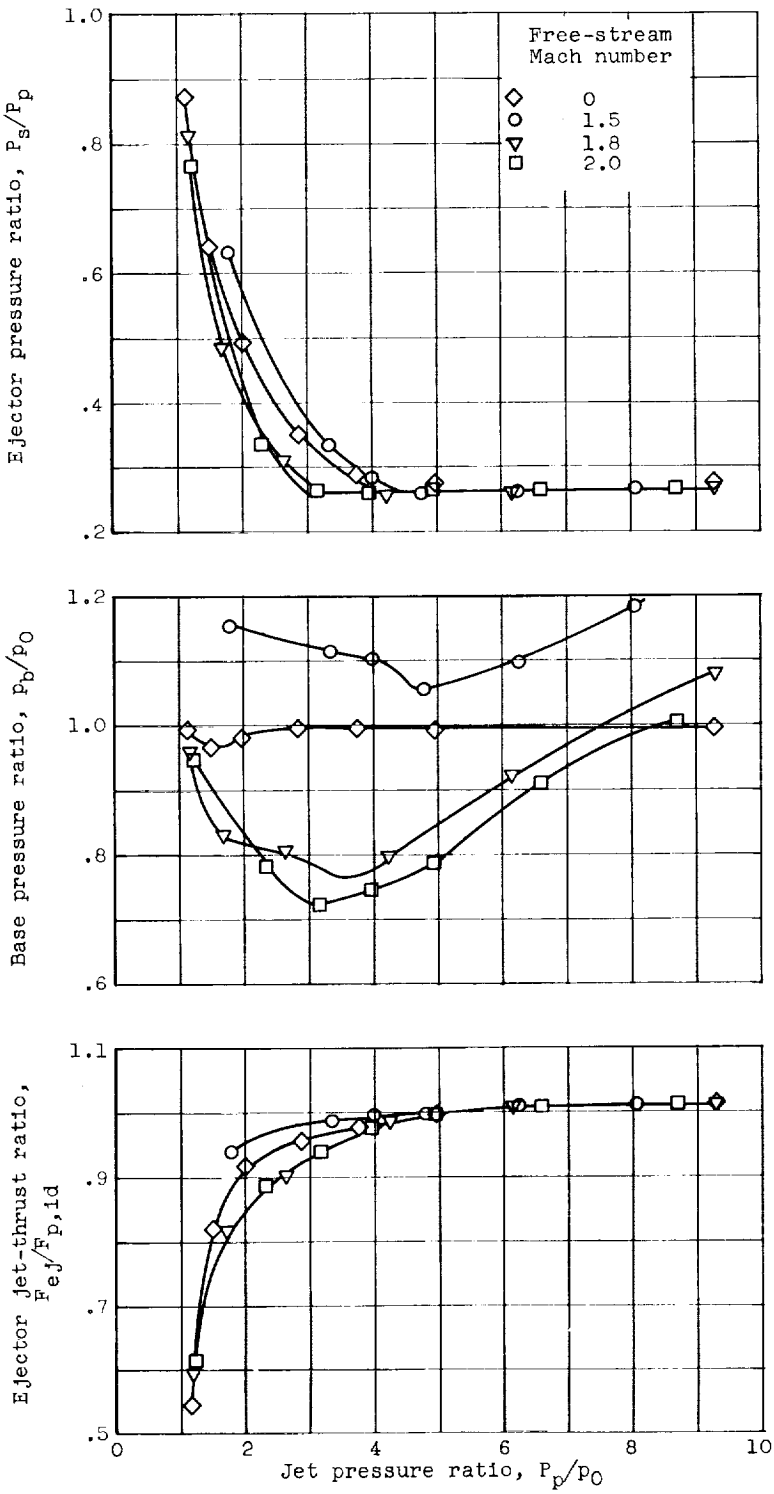

(b) Corrected weight-flow ratio, 0.06.

Figure 6. - Continued. Air-handling, base-pressure, and jet-thrust variations with jet pressure ratio for ejector 1.30-1.65-0.80.

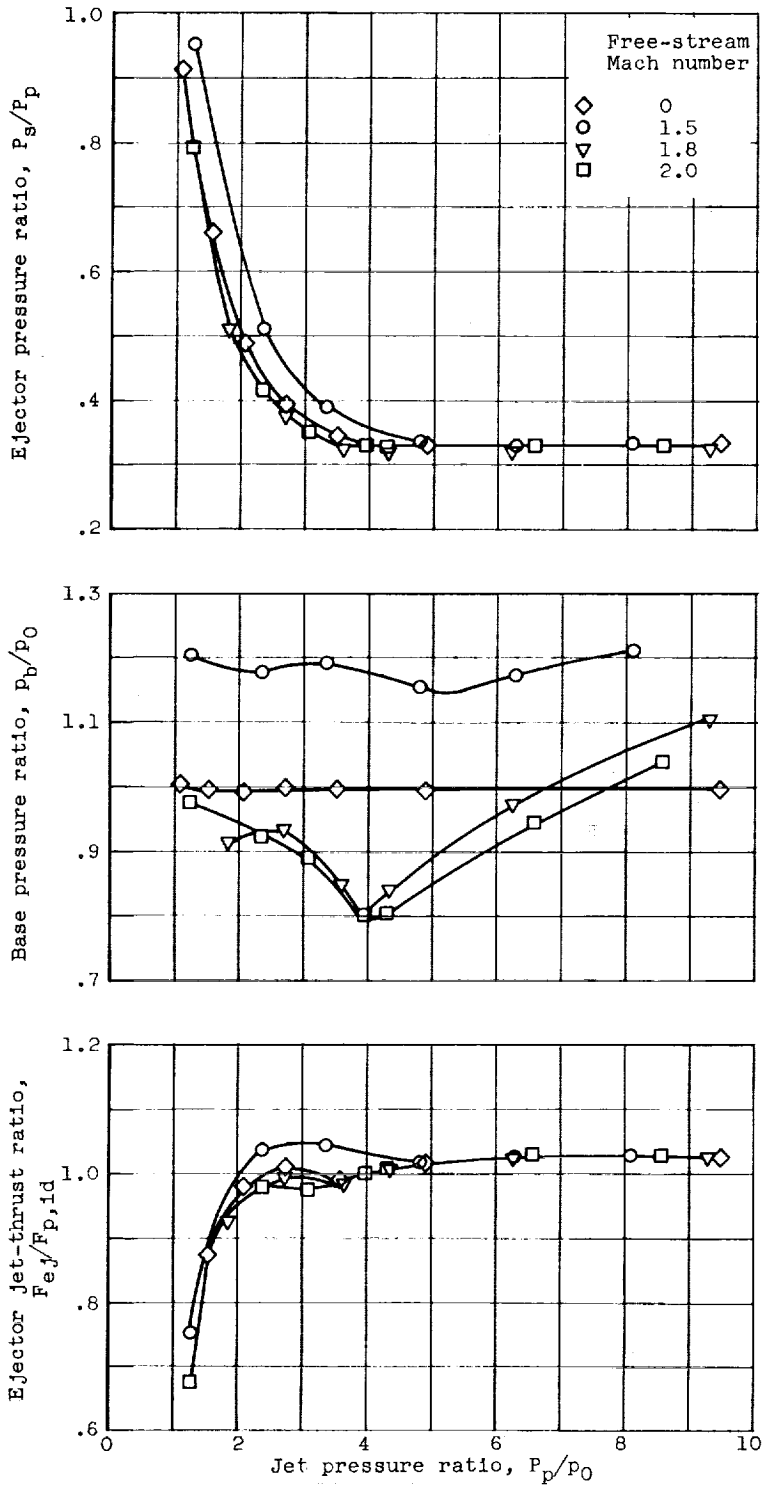

(c) Corrected weight-flow ratio, 0.13.

Figure 6. - Concluded. Air-handling, base-pressure, and jet-thrust variations with jet pressure ratio for ejector 1.30-1.65-0.80.

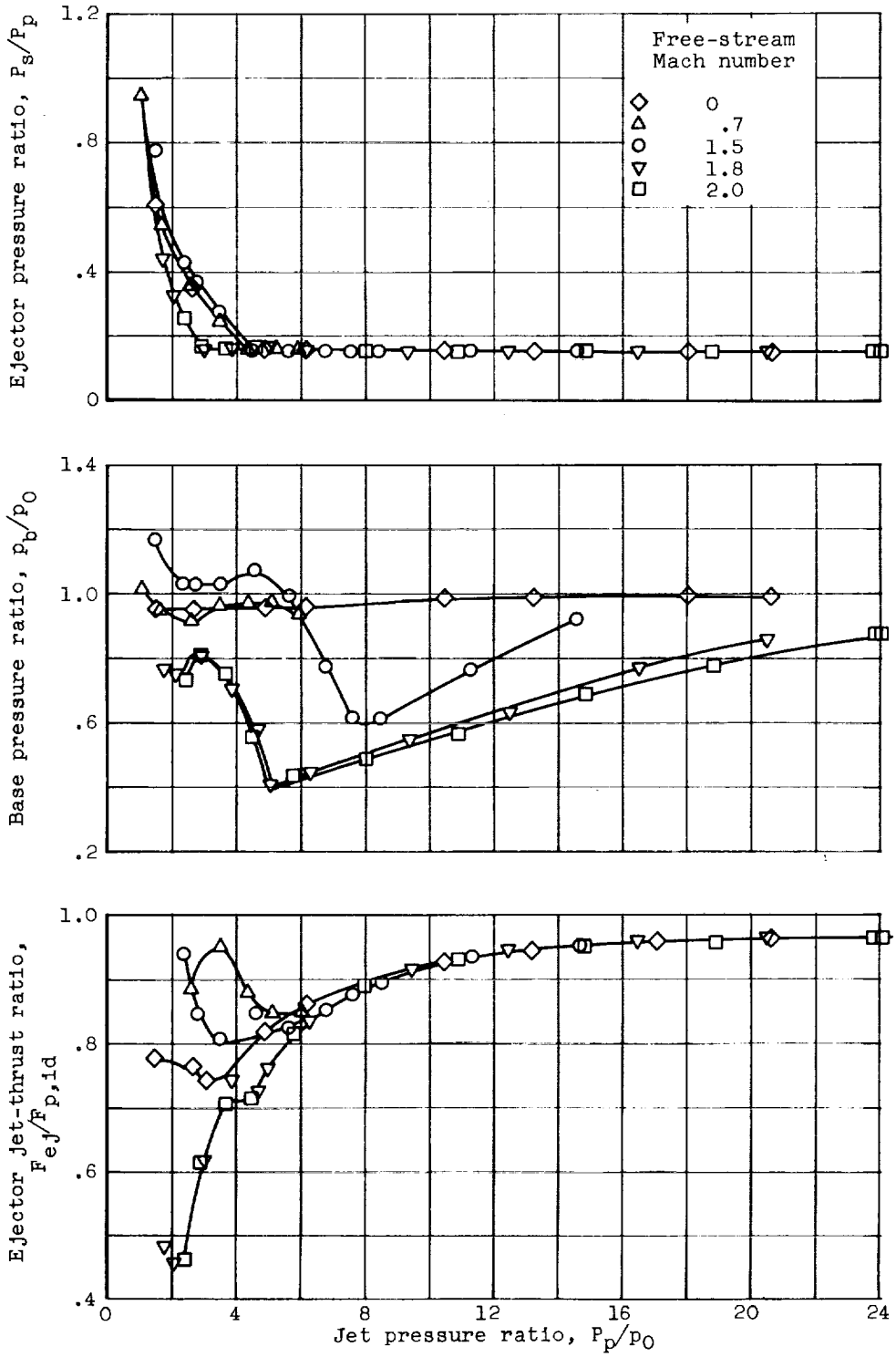

(a) Corrected weight-flow ratio, 0.

Figure 7. - Air-handling, base-pressure, and jet-thrust variations with jet pressure ratio for ejector 1.81-1.21-1.90.

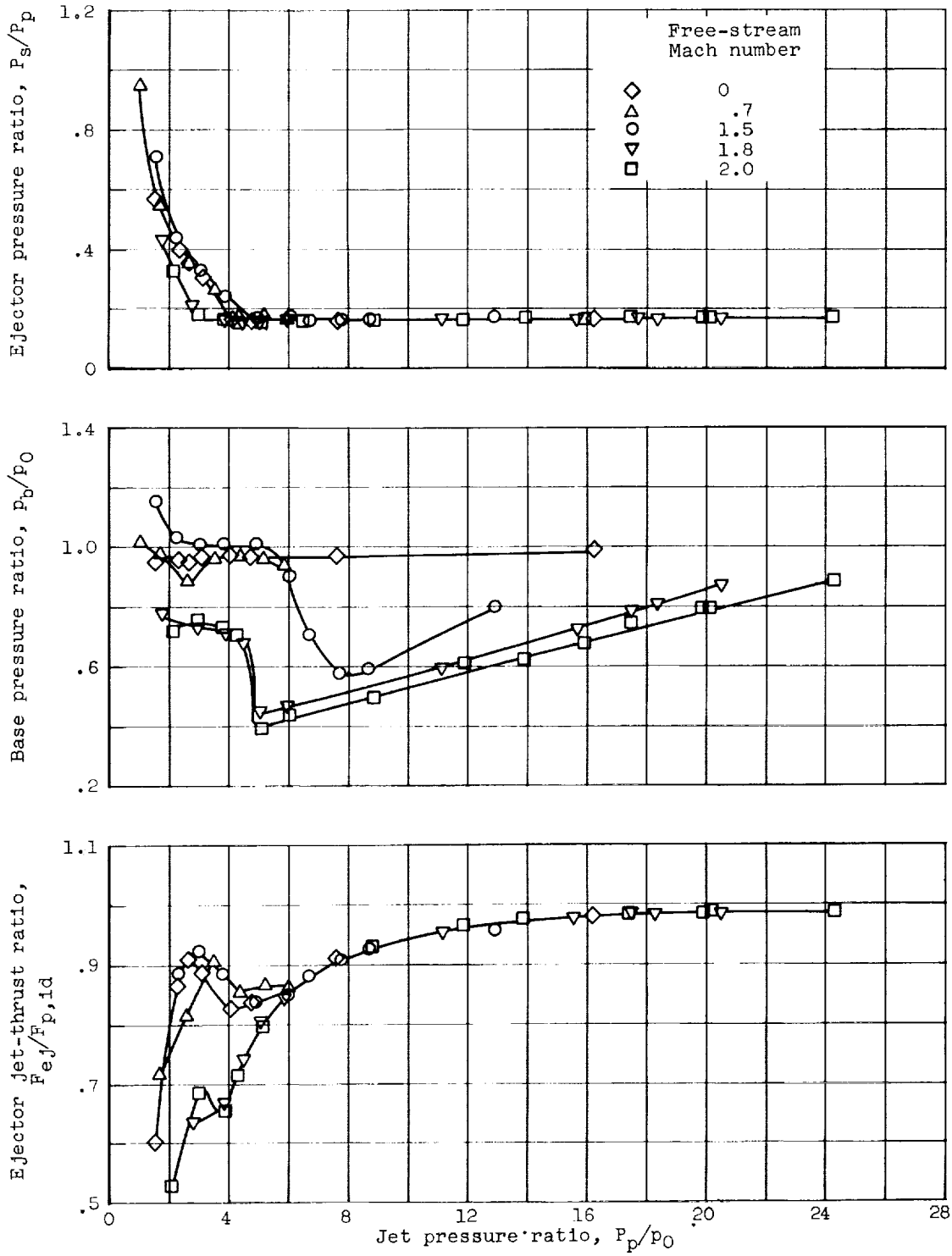

(b) Corrected weight-flow ratio, 0.03.

Figure 7. - Continued. Air-handling, base pressure, and jet-thrust variations with jet pressure ratio for ejector 1.81-1.21-1.90.

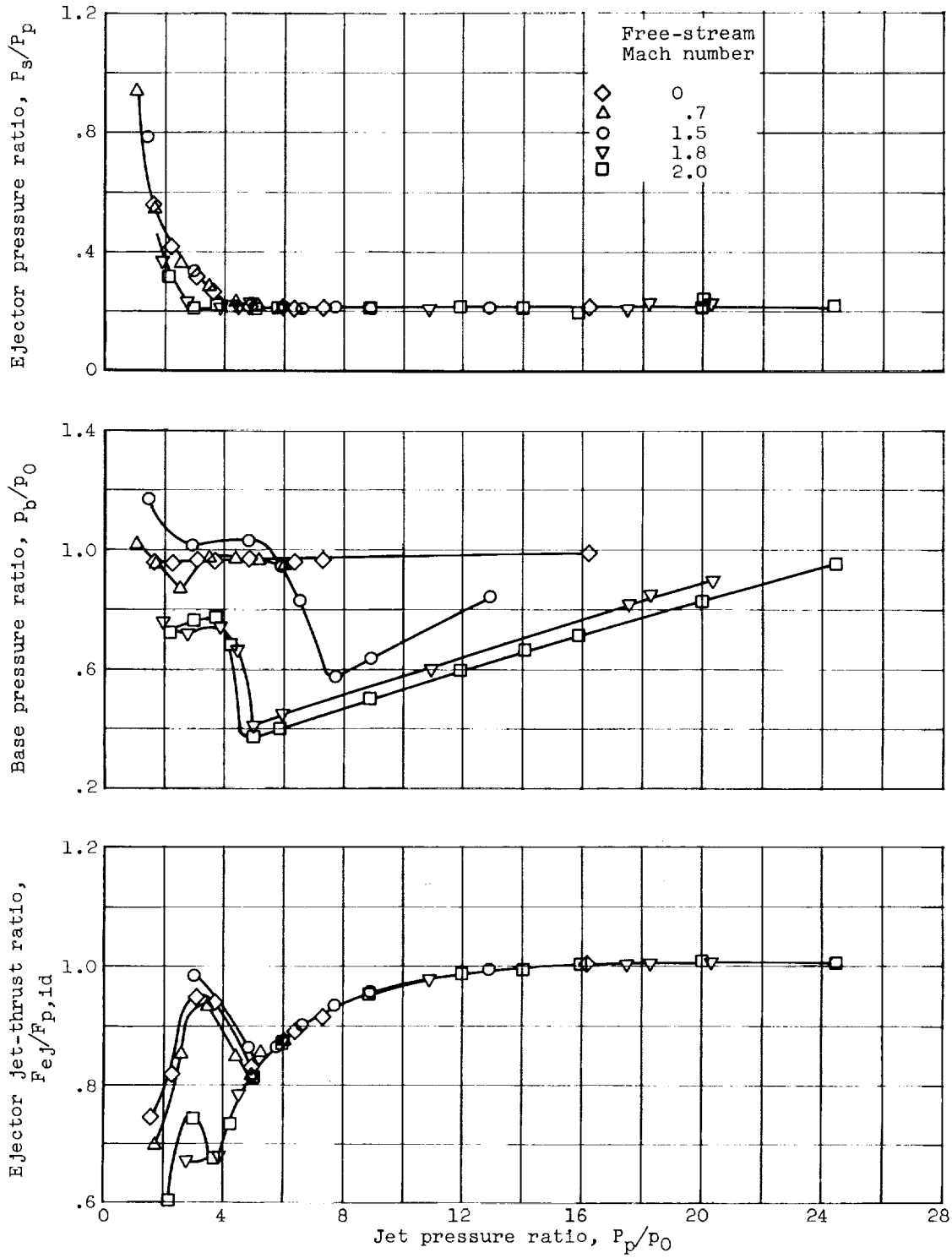

(c) Corrected weight-flow ratio, 0.05.

Figure 7. - Concluded. Air-handling, base pressure, and jet-thrust variations with jet pressure ratio for ejector 1.81-1.21-1.90.

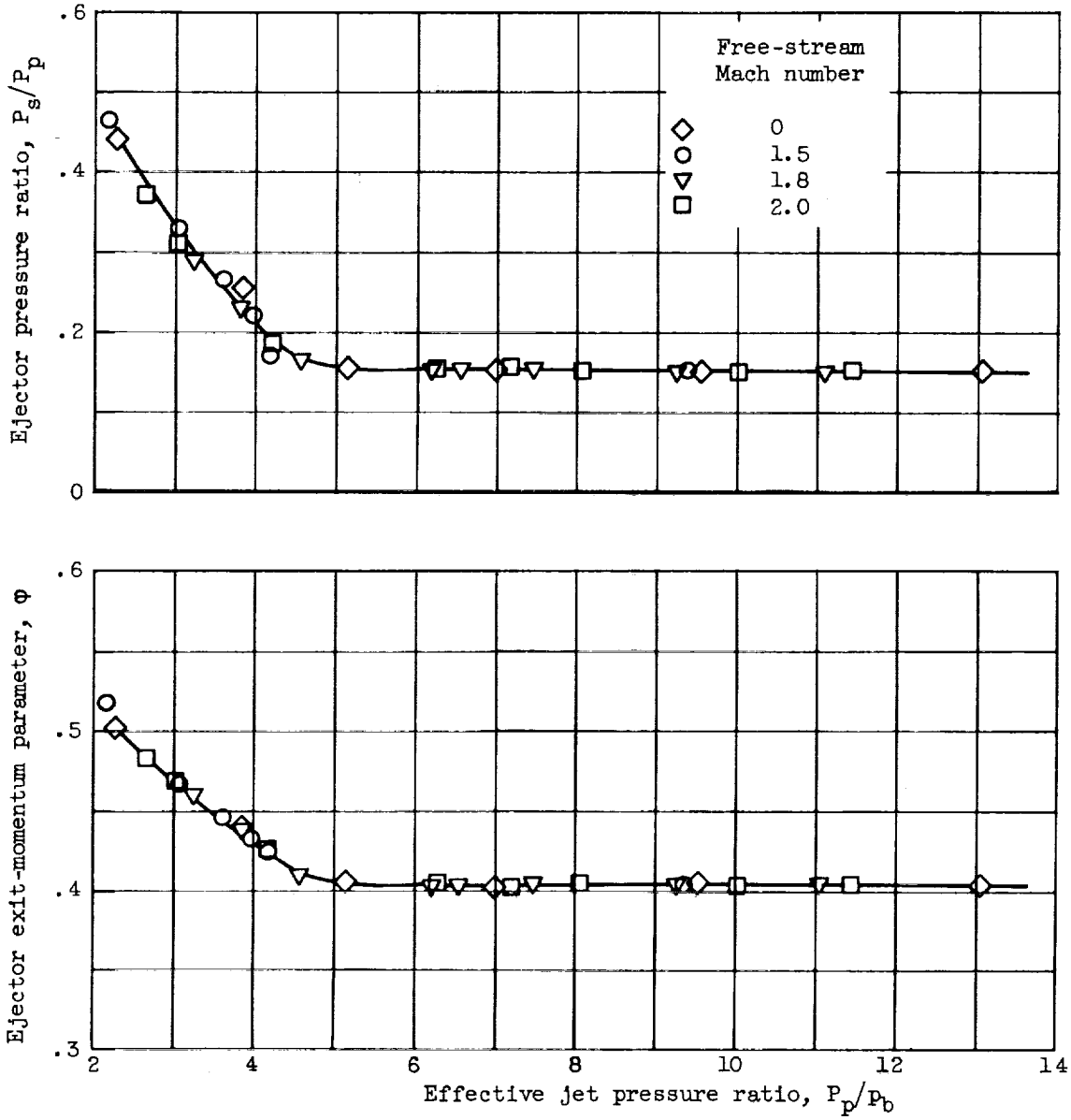

(a) Corrected weight-flow ratio, 0.

Figure 8. - Air-handling and exit-momentum variation with effective jet pressure ratio for ejector 1.45-1.80-0.80.

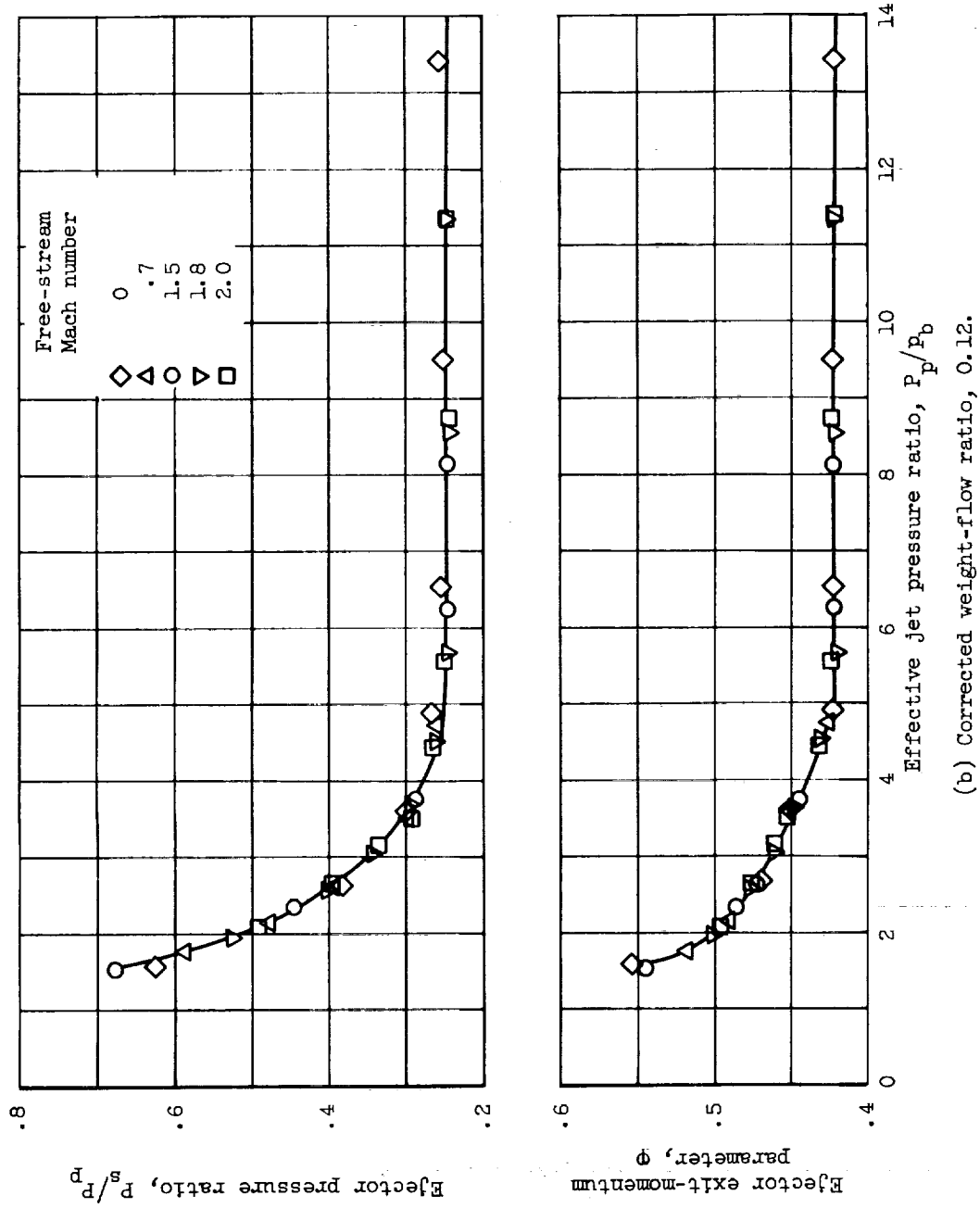

(b) Corrected weight-flow ratio, 0.12.

Figure 8. - Concluded. Air-handling and exit-momentum variation with effective jet pressure ratio for ejector 1.45-1.80-0.80.

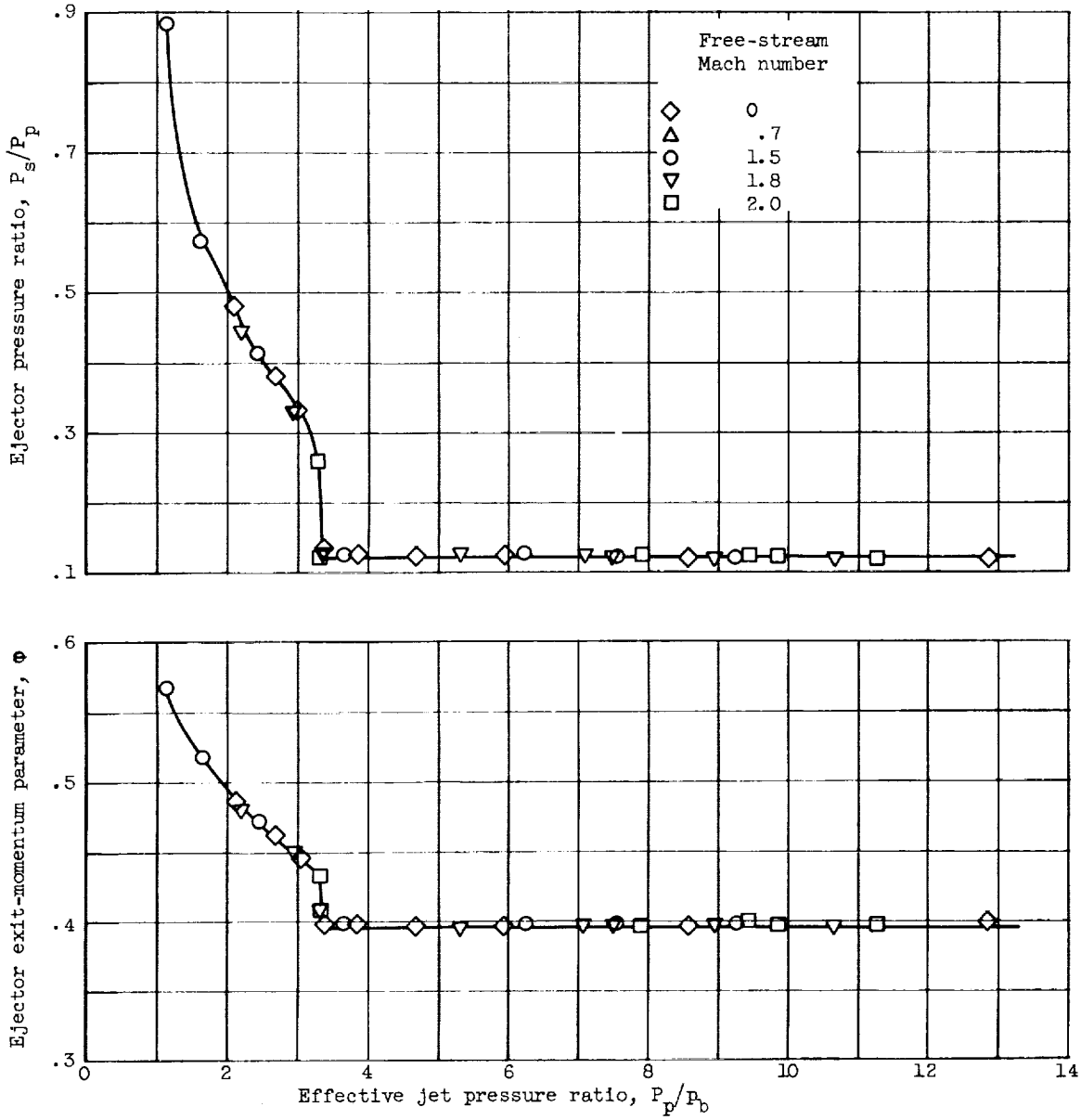

(a) Corrected weight-flow ratio, 0.01.

Figure 9. - Air-handling and exit-momentum variation with effective jet pressure ratio for ejector 1.45-1.21-0.80.

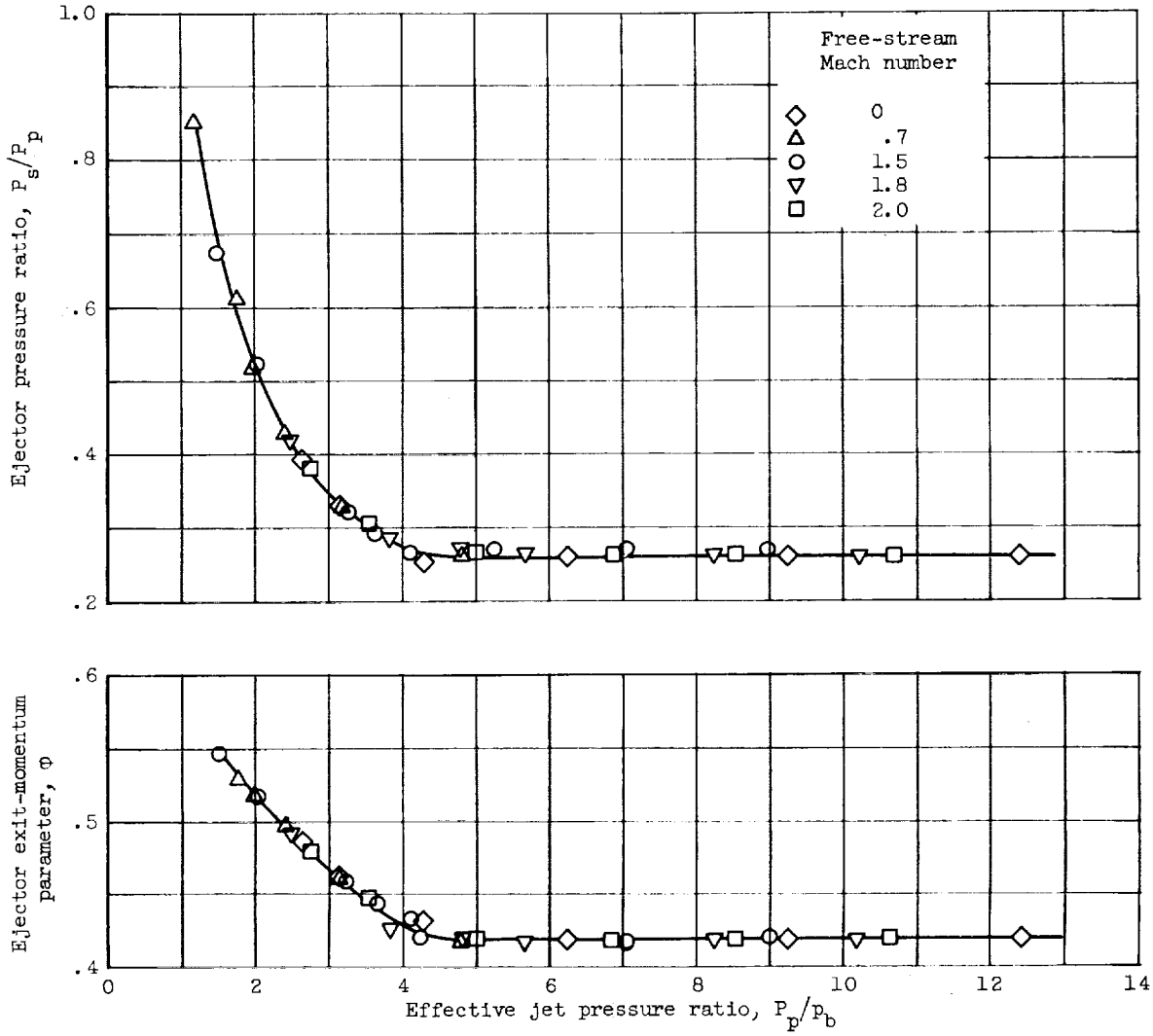

(b) Corrected weight-flow ratio, 0.05.

Figure 9. - Concluded. Air-handling and exit-momentum variation with effective jet pressure ratio for ejector 1.45-1.21-0.80.

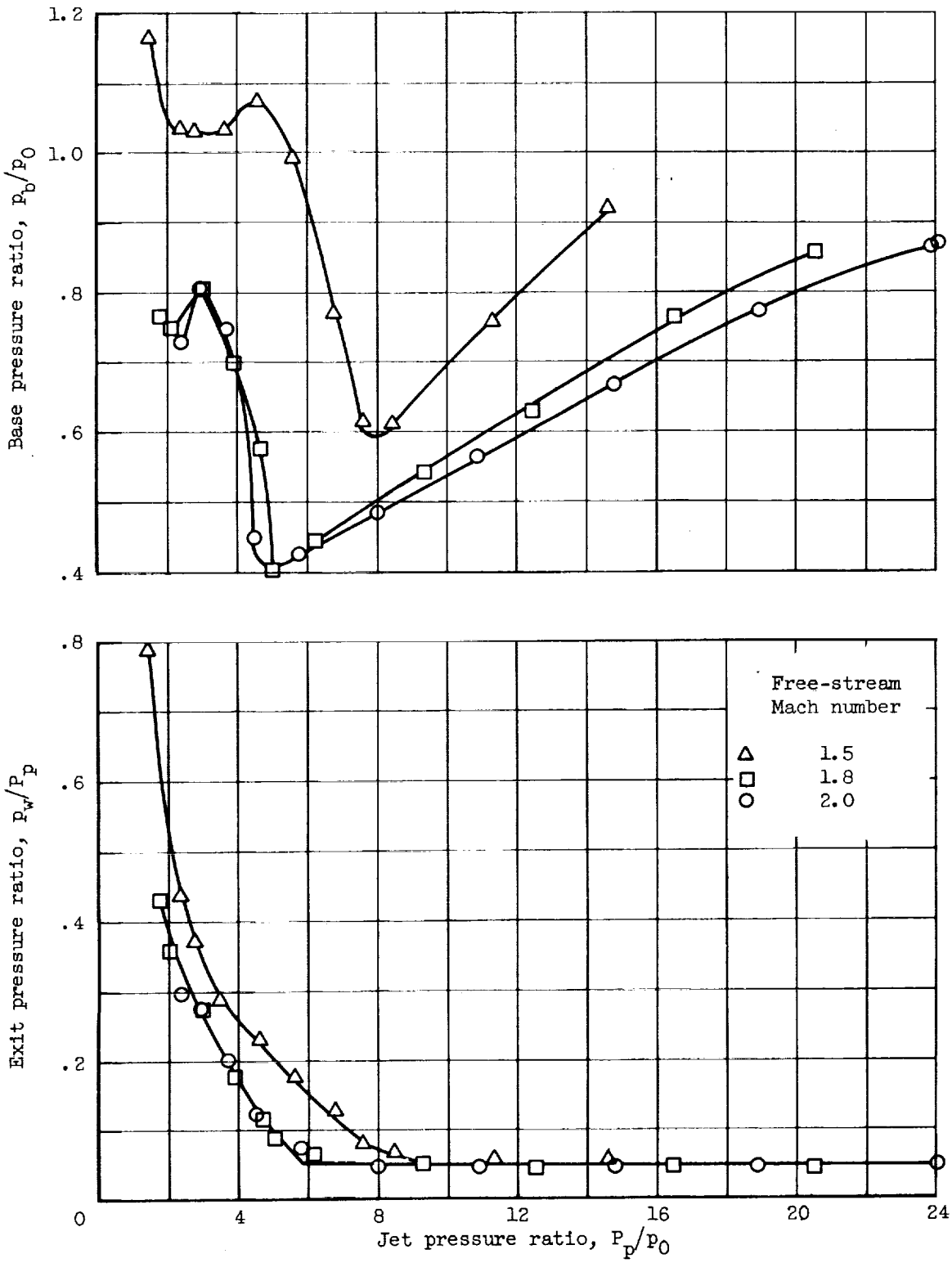

Figure 10. - Base pressure variation with ejector-exit static pressure. Ejector 1.81-1.21-1.90; corrected weight-flow ratio, 0.

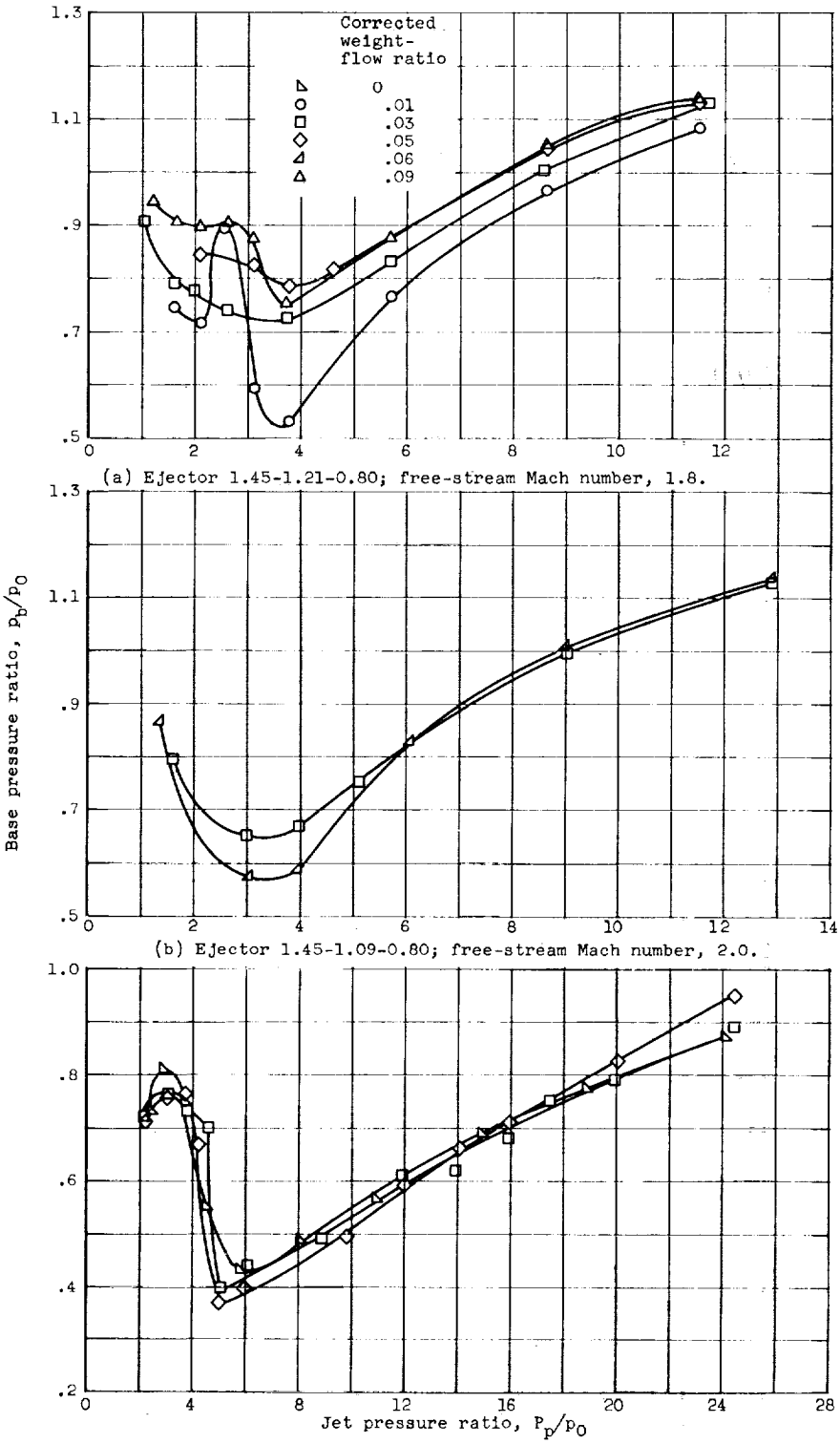

(a) Ejector 1.45-1.21-0.80; free-stream Mach number, 1.8.

(b) Ejector 1.45-1.09-0.80; free-stream Mach number, 2.0.

(c) Ejector 1.81-1.21-1.90; free-stream Mach number, 2.0.

Figure 11. - Effect of corrected weight-flow ratio on base pressure ratio.

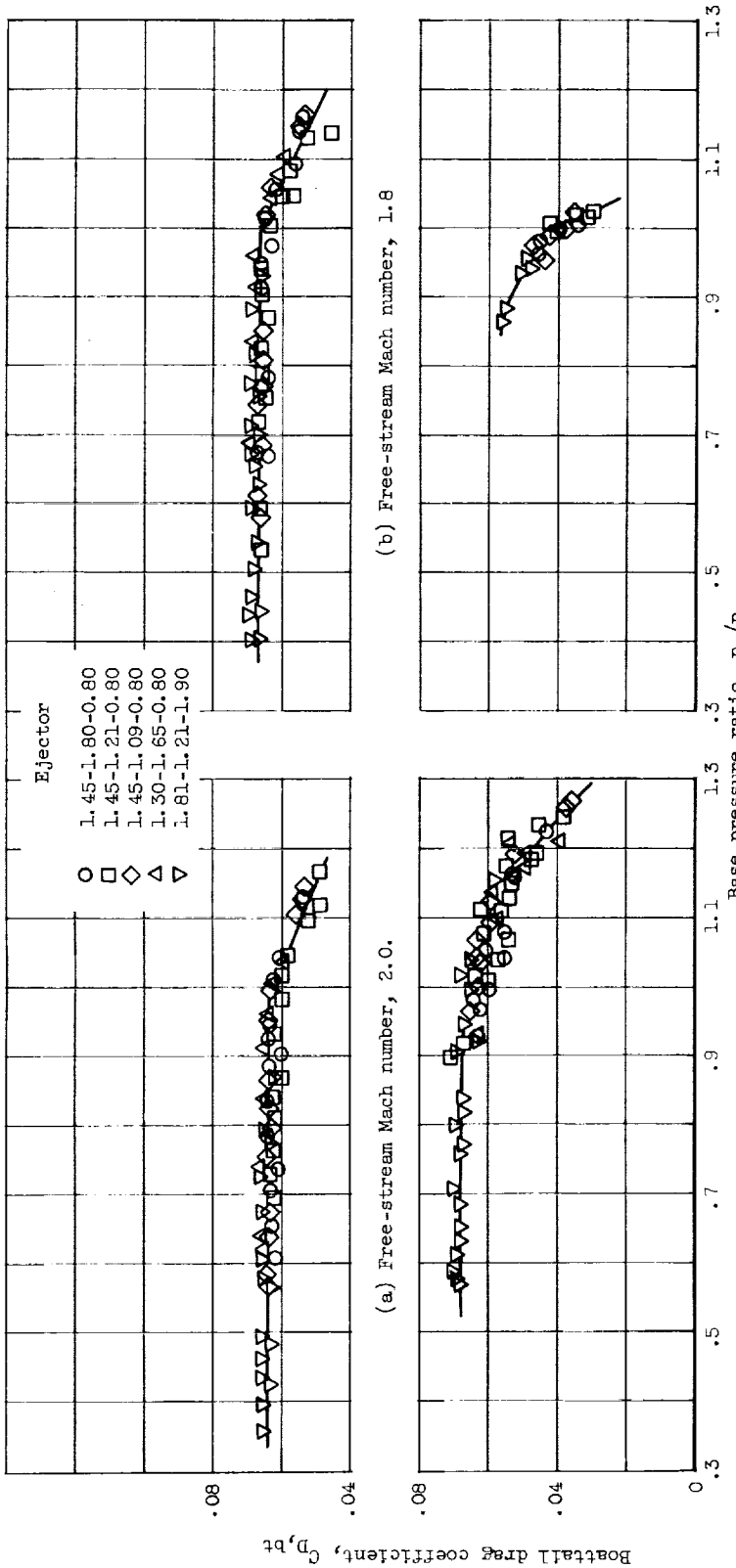

(a) Free-stream Mach number, 2.0.

(b) Free-stream Mach number, 1.8

(c) Free-stream Mach number, 1.5.

(d) Free-stream Mach number, 0.7.

Figure 12. - Effect of base pressure on boattail drag.

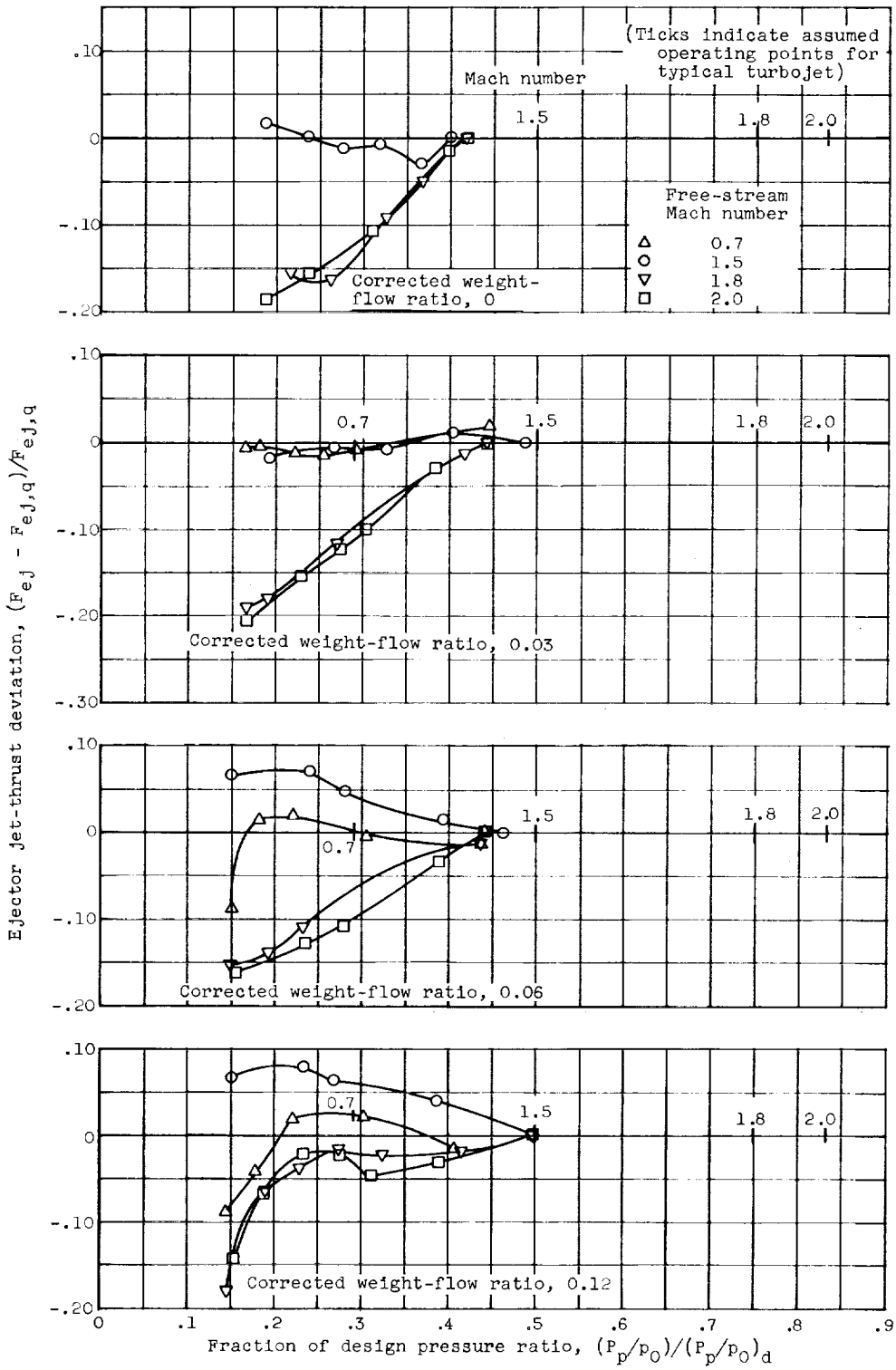

(a) Ejector 1.45-1.80-0.80.

Figure 13. - Stream effects on ejector jet-thrust performance.

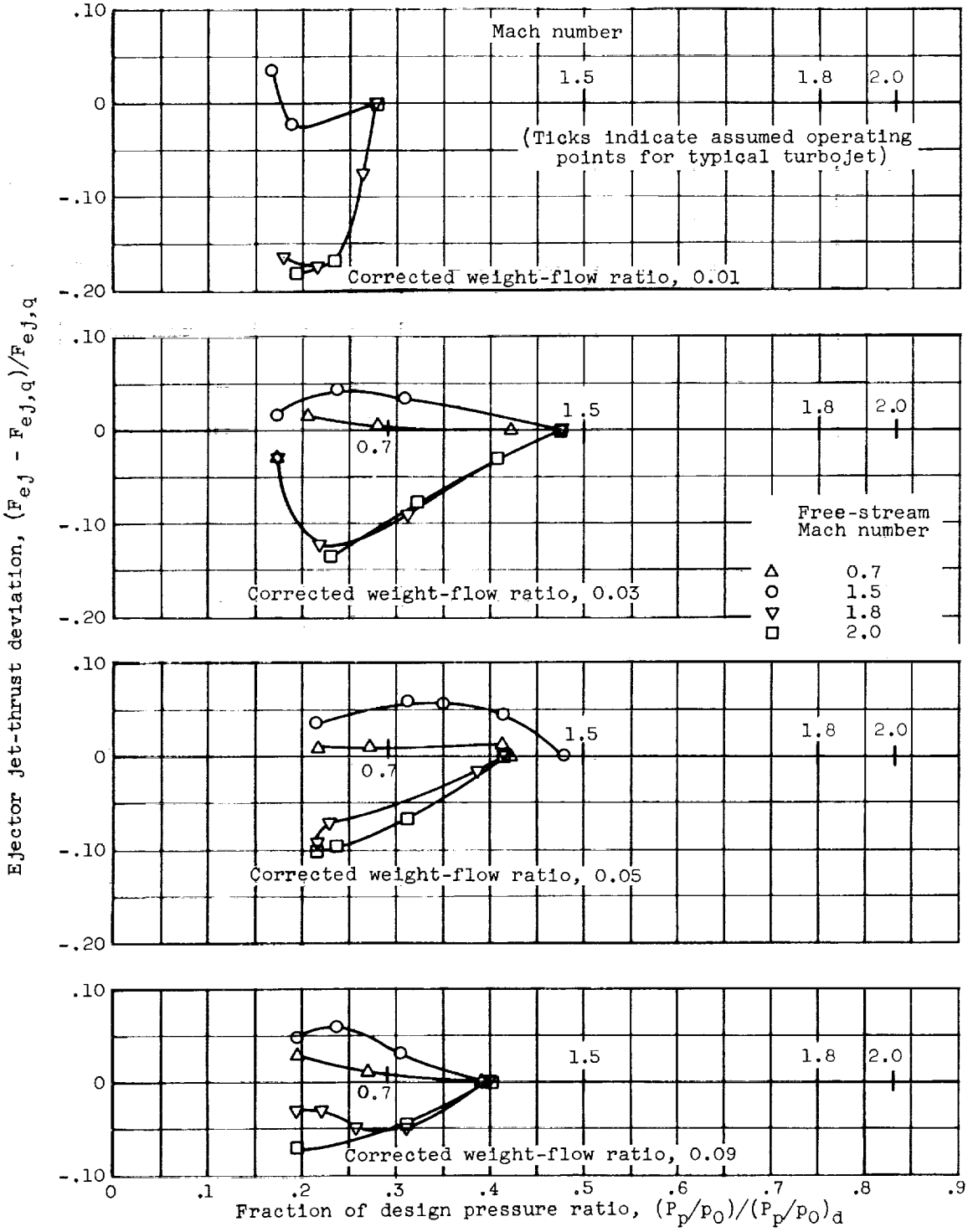

(b) Ejector 1.45-1.21-0.80.

Figure 13. - Continued. Stream effects on ejector jet-thrust performance.

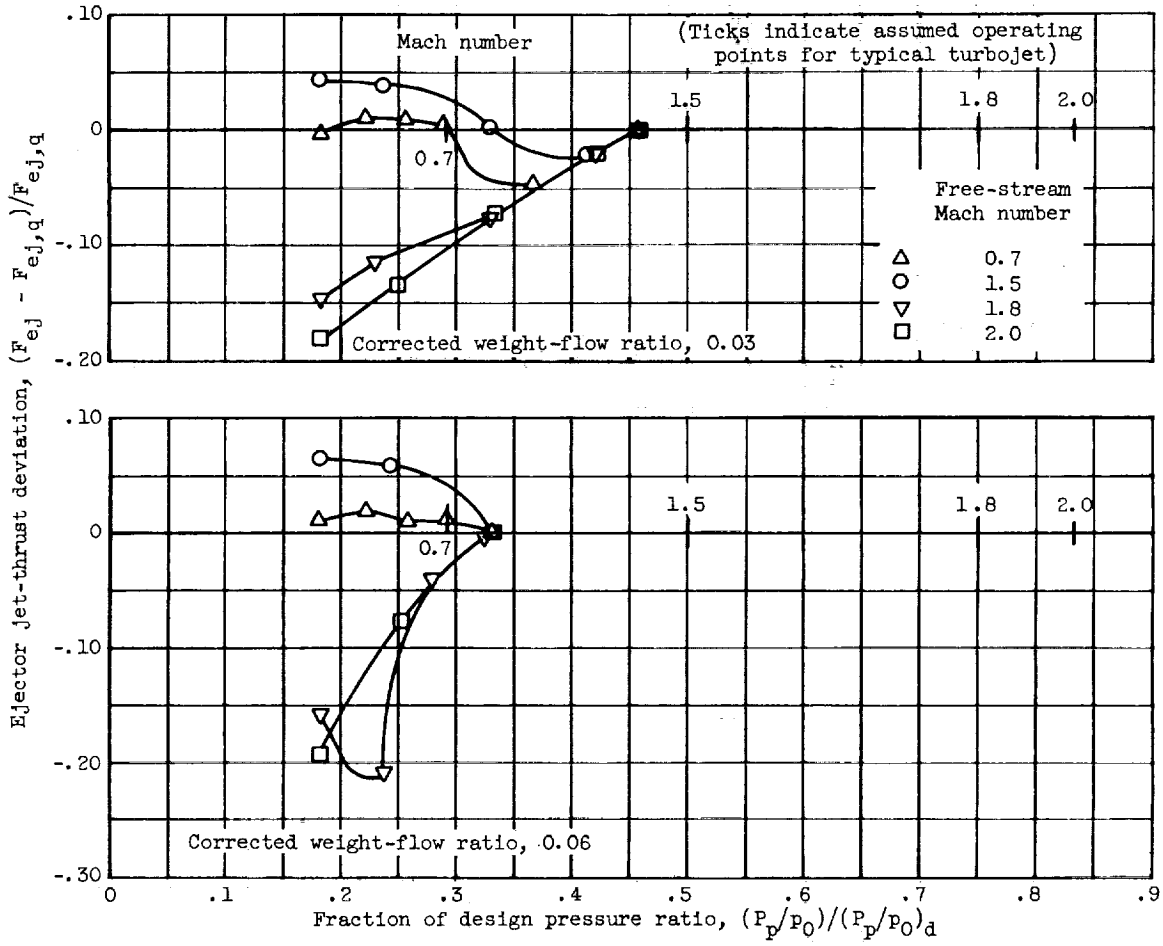

(c) Ejector 1.45-1.09-0.80.

Figure 13. - Continued. Stream effects on ejector jet-thrust performance.

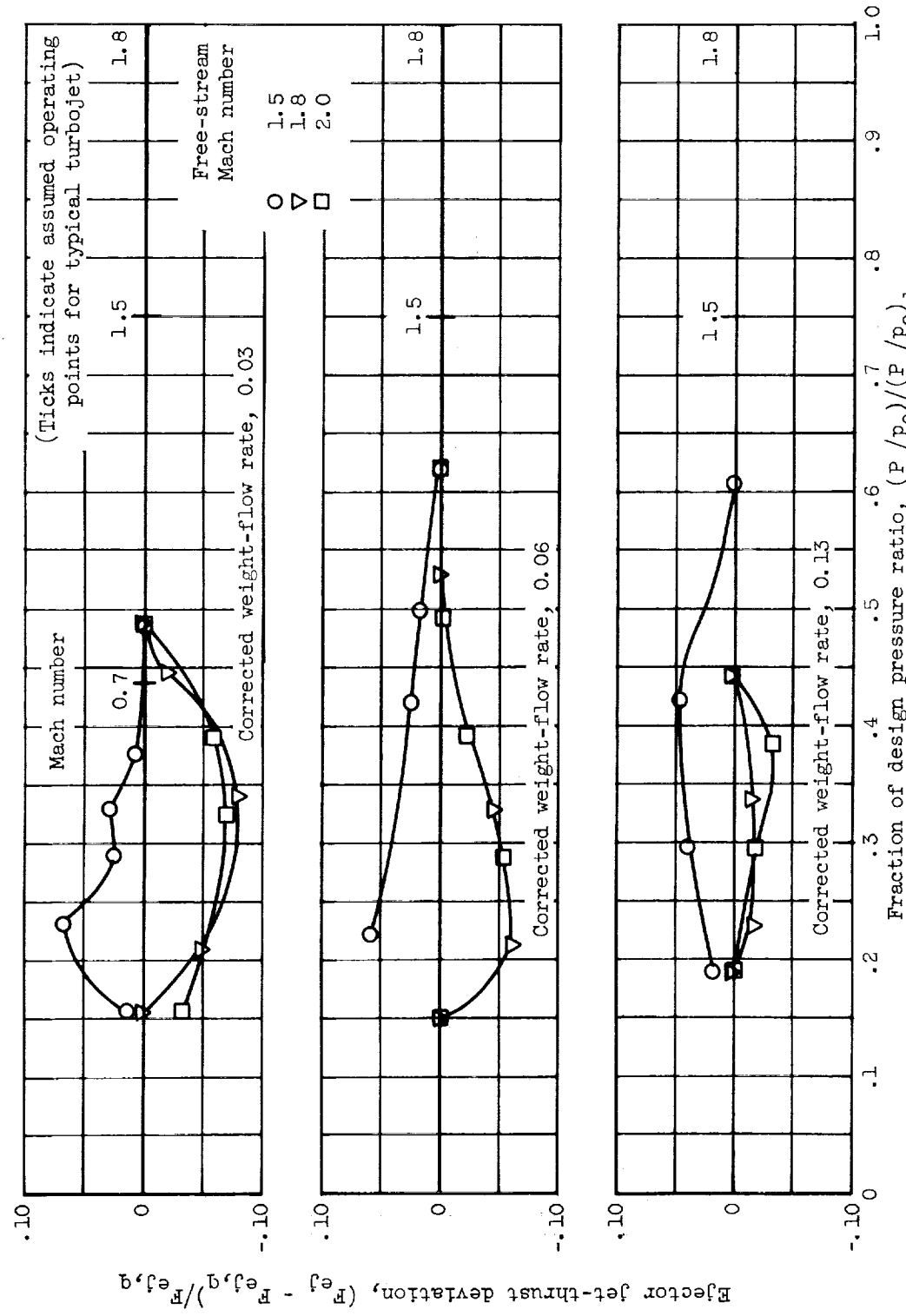

(d) Ejector 1.30-1.65-0.80.

Figure 13. - Continued. Stream effects on ejector jet-thrust performance.

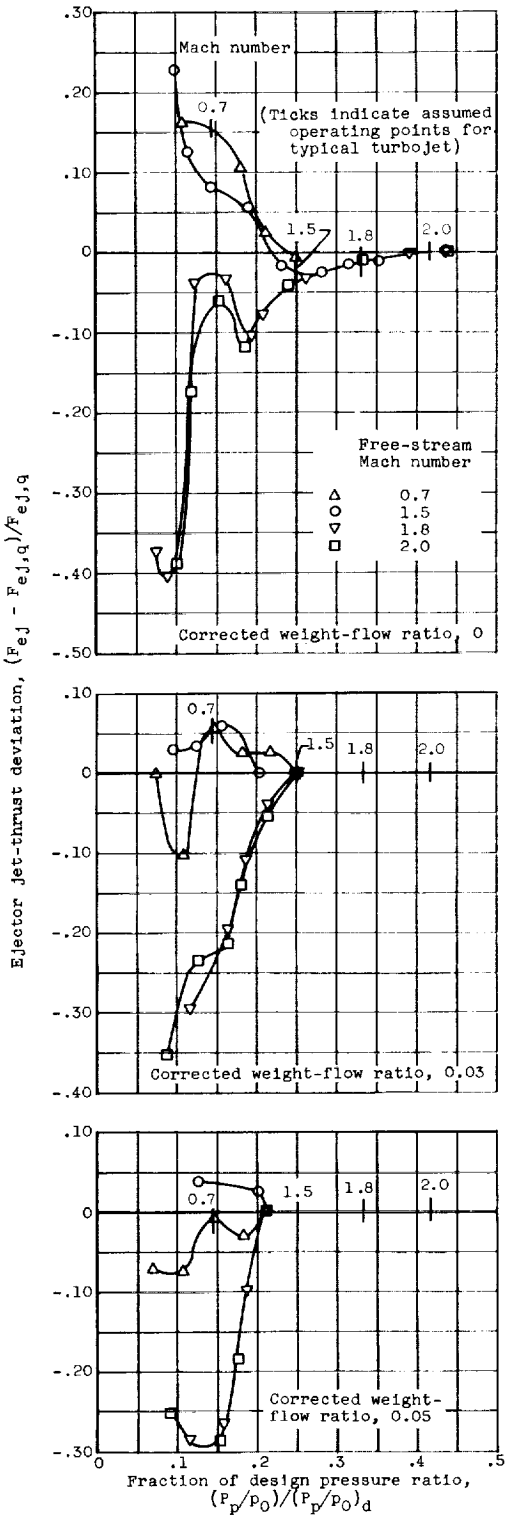

(e) Ejector 1.81-1.21-1.90.

Figure 13. - Concluded. Stream effects on ejector jet-thrust performance.